



Prospect of Relativistic Laser Plasmas for Studying Fundamental Processes and Relativistic Astrophysics

S. V. Bulanov

*Advanced Photon Research Center,
Japan Atomic Energy Agency, Kizugawa-shi, Kyoto-fu, Japan*

The 3rd International Conference on Ultrahigh Intensity Lasers:
Development, Science and Emerging Applications
(ICUIL'08 Conference)

October 27-31
Shanghai-Tongli, China

Acknowledgments

M. Borghesi

L.-M. Chen

H. Daido

T. Esirkepov

Y. Fukuda

D. Habs

M. Kando

T. Kawachi

Y. Kato

H. Kiriyama

J. Koga

J. Ma

G. Mourou

A. Pirozhkov

F. Pegoraro

T. Tajima

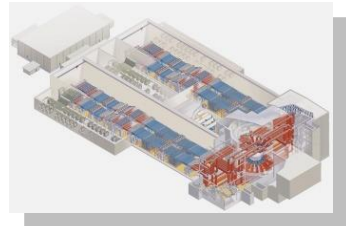
OUTLINE

- 1. Lasers and Astrophysics**
- 2. Shock Waves**
- 3. Reconnection of Magnetic Field Lines & Vortex Patterns**
- 4. Relativistic Rotator**
- 5. Flying Mirror for Femto-, Atto-, ... Super Strong Fields**
- 6. Overdense Accelerating Mirror**
- 7. Conclusion**

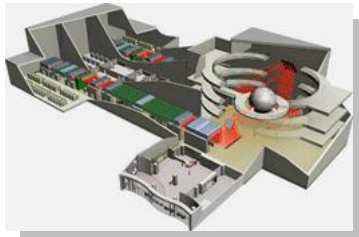
-
-
-
-
-
-
-
-
- a) V. S. Berezinskii, S. V. Bulanov, V. L. Ginzburg, V. A. Dogiel, V. S. Ptuskin,
Astrophysics of cosmic rays. (North Holland Publ.Co. Elsevier Sci. Publ. Amsterdam, 1990)
 - b) G.Mourou, T.Tajima, S.V.Bulanov, Optics in the Relativistic Regime, Rev. Mod. Phys. 78, 309 (2006)

1. Lasers and Astrophysics

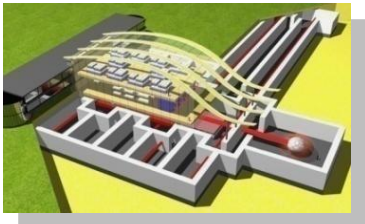
NIF



HiPER

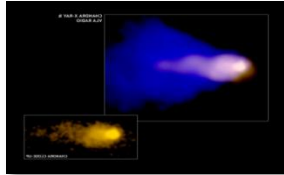


ELI

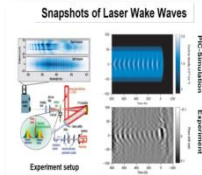


Wake

The Mouse Pulsar

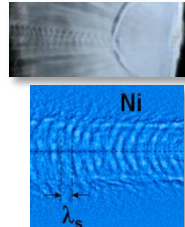


Electron Wake



Mattis et al, (2006)

Ion Wake
experiment



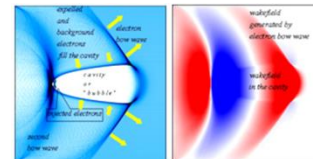
Borghesi, et al, (2005)

Bow Wave

Chandra image of M87



Electron Bow Wave



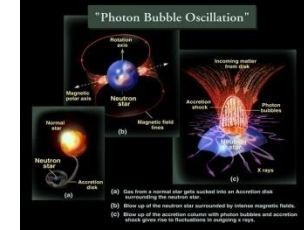
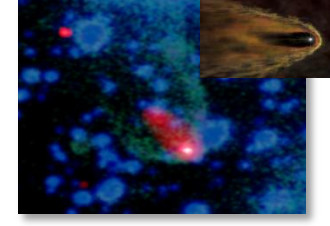
Esfirkev et al (2008)

"Kalmar" Submarine

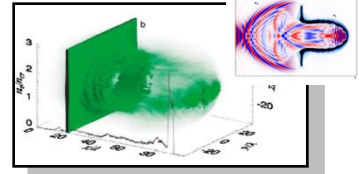


Photon Bubbles

"Black Widow" pulsar



RPDA



Esfirkev et al (2004)

Relativistic Limit in EM Wave – Plasma Interaction

Quiver energy of electron oscillating in the EM wave with the amplitude E_0 and frequency ω becomes larger than $m_e c^2$ when the dimensionless amplitude of the EM wave is greater than unity:

$$a_0 = \frac{eE_0}{m_e \omega c} > 1$$

In the EM wave interaction with the electron in vacuum its electron energy scales as (Landau & Lifshitz)

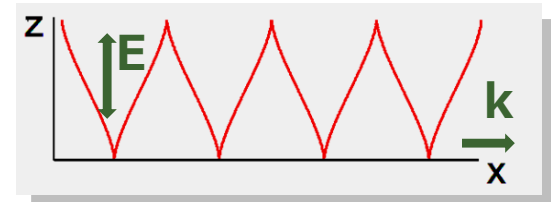
$$\mathcal{E} = \frac{1}{2} m_e c^2 a_0^2$$

When the electron oscillates in the EM wave propagating in a plasma we have (Akhiezer & Polovin)

$$\mathcal{E} = m_e c^2 a_0$$

Laser: Condition $a_0 > 1$ corresponds for $1\mu\text{m}$ laser wavelength to the intensity above $1.35 \times 10^{18} \text{ W/cm}^2$

Today's lasers can provide the intensity $I > 2 \times 10^{22} \text{ W/cm}^2$, i. e. $a_0 \approx 100$



Magneto-dipole Radiation of Oblique Rotator

Space: Magneto-dipole radiation of oblique rotator, has been considered as a model for the pulsar radiation

Power emitted by rotator is given by
$$W = \frac{2}{3} \frac{\mu^2 (\sin \theta)^2 \omega^4}{c^3}$$

Magnetic moment: $\mu \approx B r_p^3$; θ is the angle between $\vec{\mu}$ and $\vec{\omega}$

The EM wave intensity at the distance r is $I = W / 4\pi r^2$

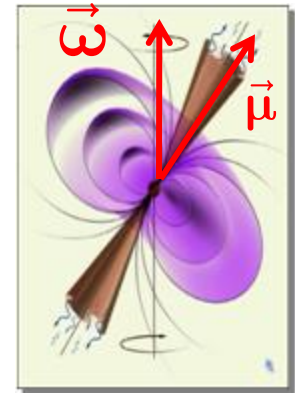
In the wave zone, $r = c / \omega$, the dimensionless wave amplitude is

$$a_0 = \frac{e \mu \omega^2}{m_e c^4}$$

For typical values of magnetic field, $B = 10^{12} G$, rotation frequency, $\omega = 200 s^{-1}$,

and pulsar radius: $r_p = 10^6 cm$

it yields $\mu = 10^{30} G cm^3$ and $a_0 \approx 10^{10}$

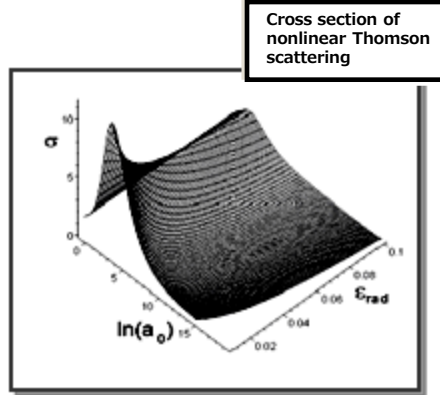


(Michel;
Beskin, Gurevich, Istomin)



Crab pulsar

Amplitude	Intensity	Regime
$a_0 = \frac{eE_0}{m_e c \omega}$	$\left[\frac{\text{W}}{\text{cm}^2} \right]$	
$a_{QED} = \frac{m_e c^2}{\hbar \omega}$	2.4×10^{29}	e^+, e^- in vacuum
$a_{QM} = \frac{2e^2 m_e c}{3 h^2 \omega}$	5.6×10^{24}	quantum effects
$a_p = \frac{m_p}{m_e}$	1.3×10^{24}	relativistic p
$a_{rad} = \left(\frac{3\lambda}{4\pi r_e} \right)^{1/3}$	1×10^{23}	radiation damping
$a_{rel} = 1$	1.3×10^{18}	relativistic e^-

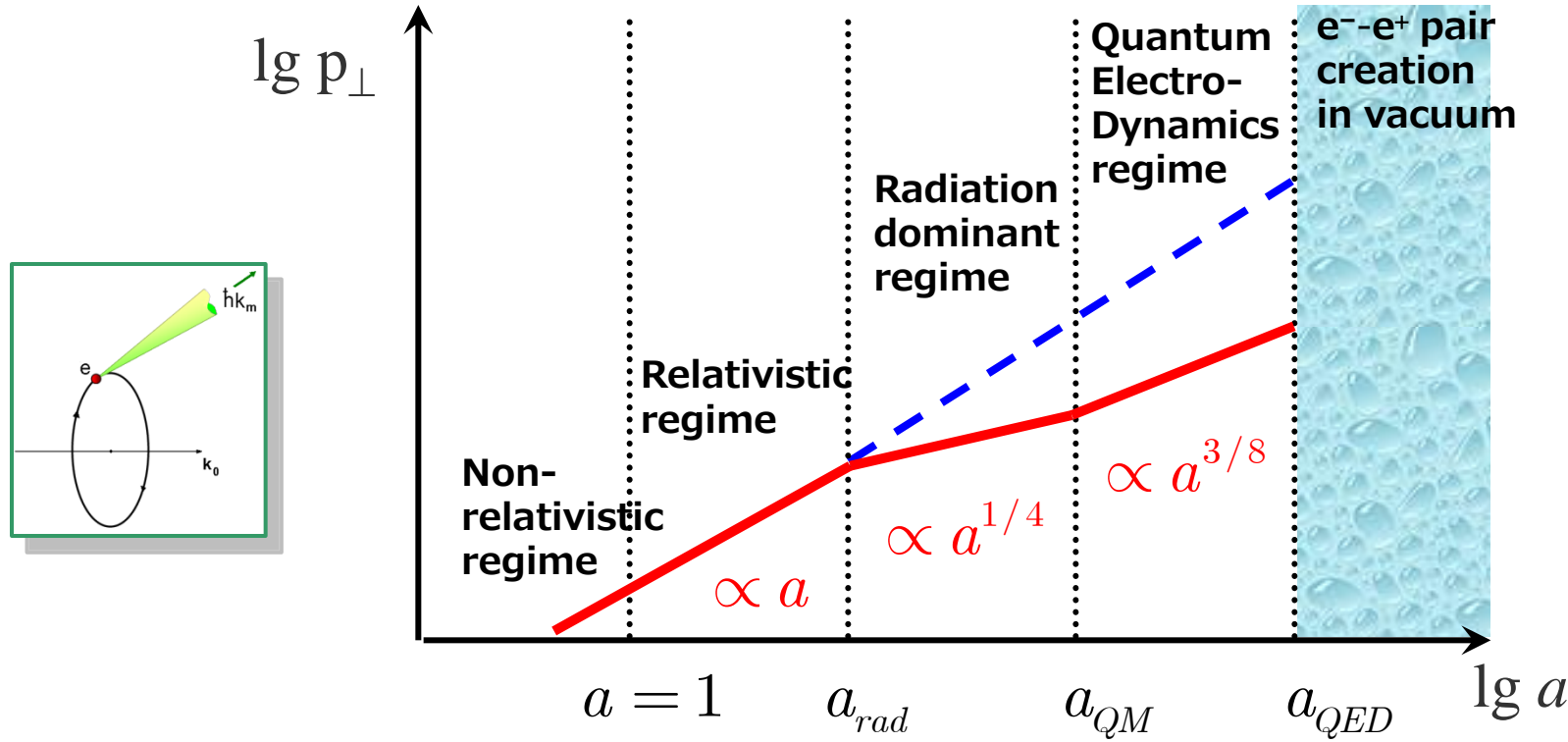


Ya. B. Zel'dovich, 1975; A.G.Zhidkov, et al., 2003
SVB, T. Zh. Esirkepov, J. Koga, T. Tajima, 2004

For the Crab pulsar,
 $\omega = 200 s^{-1}$, $a_0 = 10^{10}$
the radiation damping effects are crucially important because the EM wave amplitude is above the threshold:

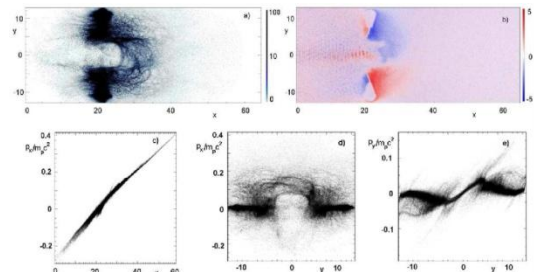
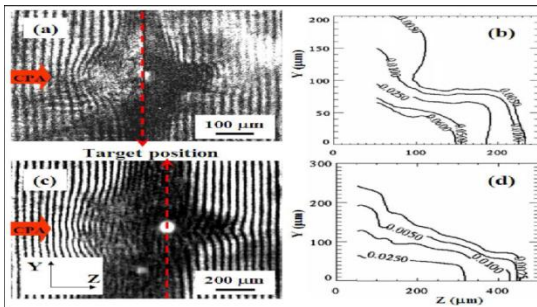
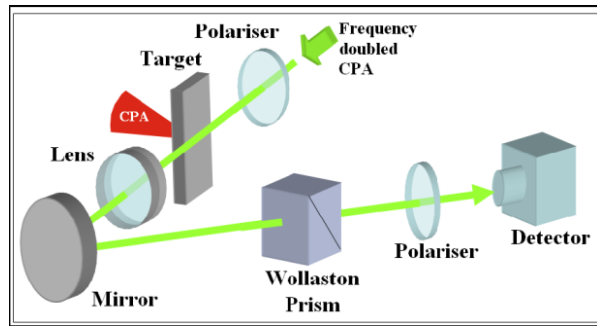
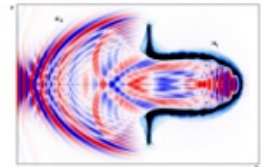
$$a_{rad} = \left(\frac{3\lambda}{4\pi r_e} \right)^{1/3} = 10^7$$

Laser-Plasma Interaction in the “Radiation-Dominant” Regime



Plasma jets driven by Ultra-intense laser interaction with thin foils

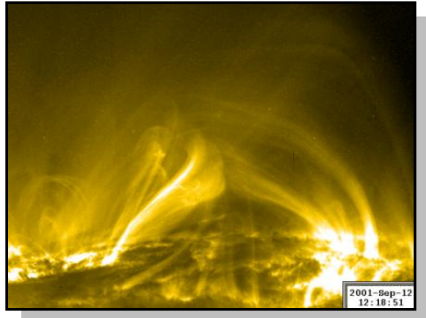
VULCAN Nd-glass laser of Rutherford Appleton laboratory,
(60 J, 1ps & 250 J, 0.7 ps) interacts with foils (3, 5 μm , Al & Cu)



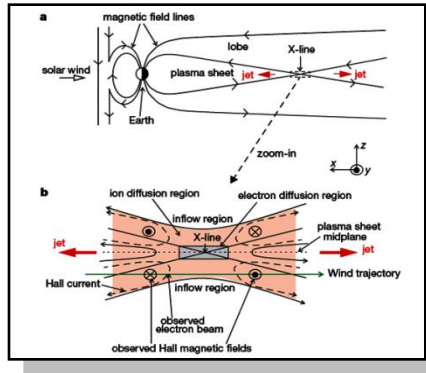
$$\frac{p^{(0)}}{m_p c} = \frac{2W(W+1)}{2W+1} \approx 2W$$

$$W = \int \frac{E^2(\psi)}{2\pi n_0 l} d\psi \ll 1$$

Reconnection of Magnetic Field Lines



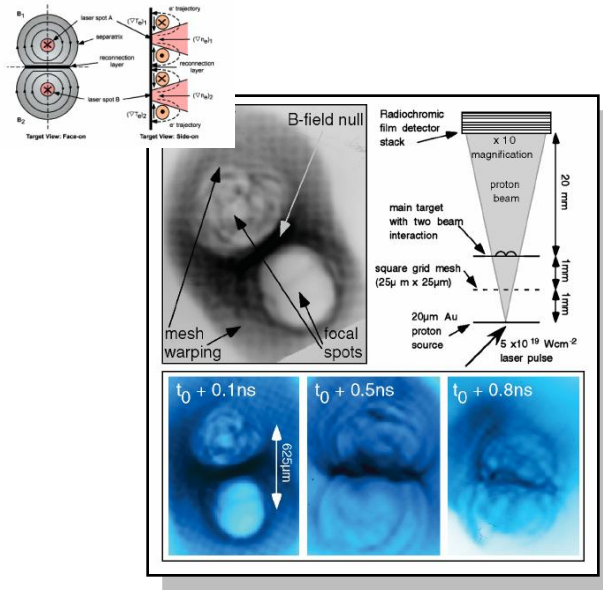
Solar flare/
12.09.2001(12:18:51)



M. Oieroset, et al.,
Nature (2001)

MAGNETIC RECONNECTION IN LASER PLASMAS HAS BEEN FORESEEN IN:

G.A.Askar'yan, SVB, F.Pegoraro, A.M.Pukhov,
Magnetic interaction of self-focused channels and magnetic wake excitation in high intense laser pulses,
Comments on Plasma Physics and Controlled Fusion 17, 35 (1995).



Nilson et al, PRL 97, 255001
(2006)

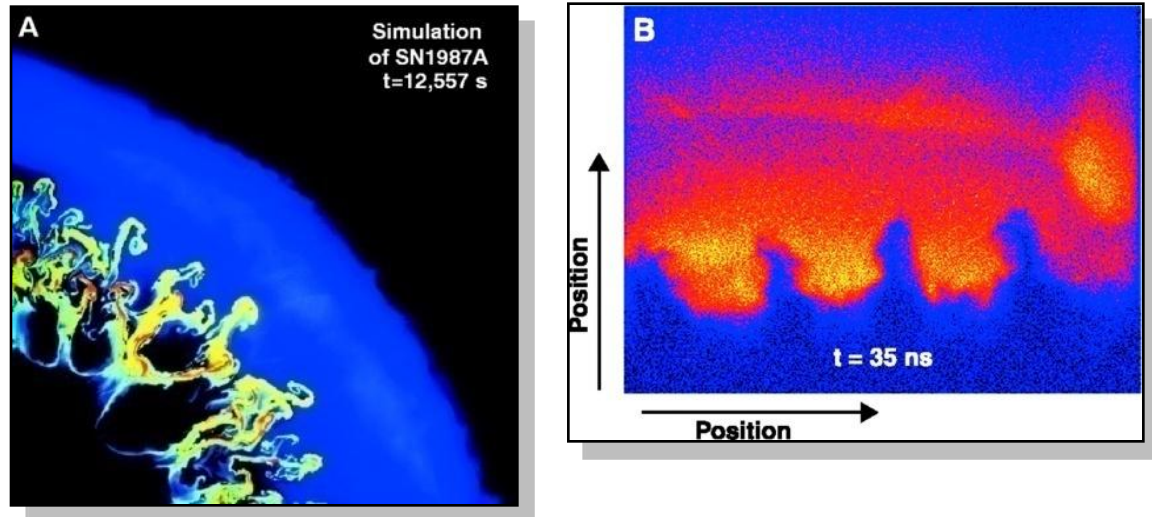
Laboratory Astrophysics

Laboratory Astrophysics



**Relativistic Laboratory
Astrophysics
with the Ultra Short Pulse
High Power Lasers**

**We deal with the collisionless
plasmas**

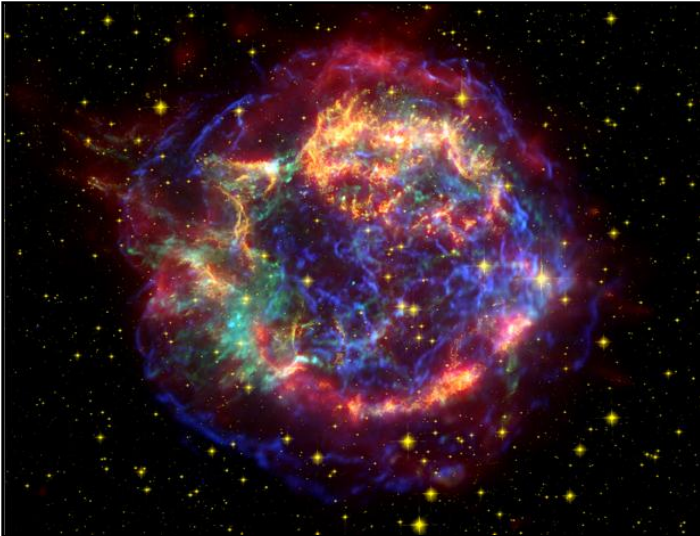


B. A. Remington et al., Science 284, 1488 (1999)

*Rayleigh-Taylor & Richtmayer-Meshkov Instability,:
seen in simulations of Supernovae (right) and
in laser irradiated Nuclear Fusion target*

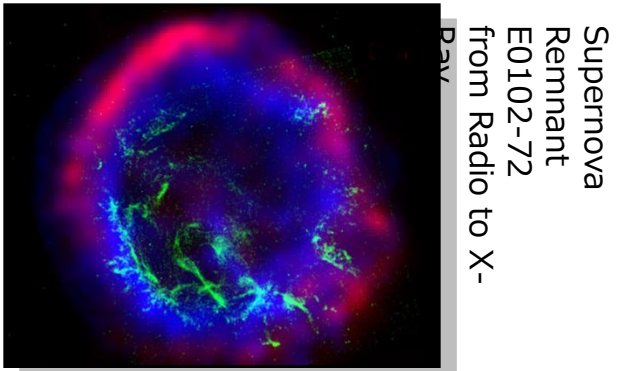
Radiative shock waves, plasma jets

2. Shock Waves



Cassiopea A

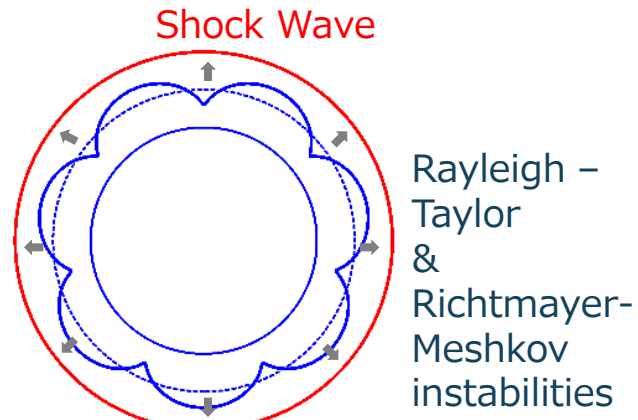
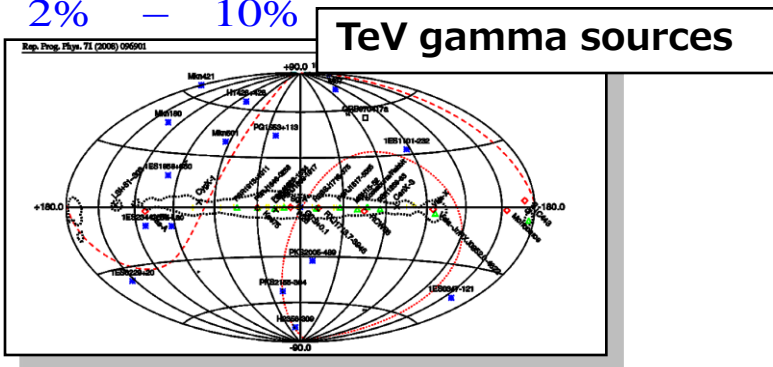
Shock Waves and RT Instability



$$\text{SNII} \quad \mathcal{E}_{tot} = 10^{52} erg$$

1/10 – 1/30 year

2% = 10%



1. Ballistic motion of the ejecta
 2. Sedov's regime:

$$R_{SW} = 1.5(\mathcal{E}_{tot} t^2 / \rho)^{1/3} = \frac{5}{2} V_{SW} t$$

$$V_{SW} \propto t^{-3/5}$$
 3. Radiation losses: $R_{SW} \propto t^{2/7}$

Collisionless Shock Waves

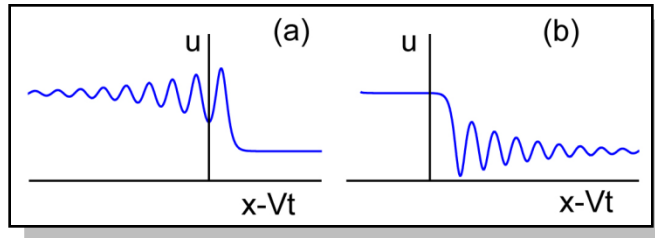
A structure of collisionless schock waves is determined by the counter play of dissipation and dispersion effects. These effects are described within the framework of the Korteweg-de Vries-Burgers equation:

$$\partial_t u + u \partial_x u - \nu \partial_{xx} u - \beta \partial_{xxx} u = 0$$

nonlinearity dispersion
dissipation

R.Z.Sagdeev, 1959

- a) MS wave
propagating
almost
perpendicularly to B field $\beta \approx$



- b) MS wave propagation is almost parallel to B field

$$\beta \approx -v_a c^2 / 2\omega_{pe}$$

with $v_a = B^2 / \sqrt{4\pi nm_p}$

Observation of Collisionless Shocks in Laser-Plasma Experiments

L. Romagnani,^{1,*} S. V. Bulanov,^{2,3} M. Borghesi,¹ P. Audebert,⁴ J. C. Gauthier,⁵ K. Löwenbrück,⁶ A. J. Mackinnon,⁷ P. Patel,⁷ G. Pretzler,⁶ T. Toncian,⁶ and O. Willi⁶

¹School of Mathematics and Physics, The Queen's University of Belfast, Belfast, Northern Ireland, United Kingdom

²APRC, JAEA, Kizugawa, Kyoto, 619-0215 Japan

³Prokhorov Institute of General Physics RAS, Moscow, 119991 Russia

⁴Laboratoire pour l'Utilisation des Lasers Intenses (LULI), UMR 7605 CNRS-CEA-École Polytechnique-Univ, Paris VI, 91128 Palaiseau, France

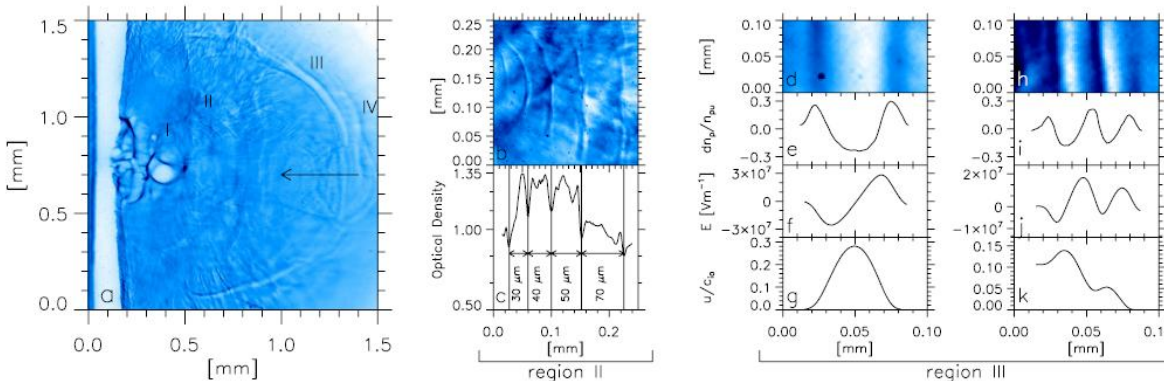
⁵Université Bordeaux 1; CNRS; CEA, Centre Lasers Intenses et Applications, 33405 Talence, France

⁶Institut für Laser- und Plasmaphysik, Heinrich-Heine-Universität, Düsseldorf, Germany

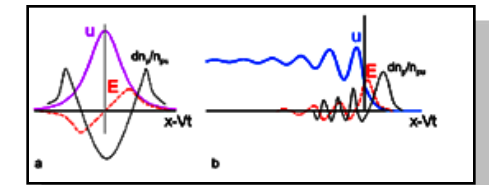
⁷Lawrence Livermore National Laboratory, Livermore, California 94550, USA

(Received 4 April 2008; published 10 July 2008)

The propagation in a rarefied plasma ($n_e \leq 10^{15} \text{ cm}^{-3}$) of collisionless shock waves and ion-acoustic solitons, excited following the interaction of a long ($\tau_L \sim 470 \text{ ps}$) and intense ($I \sim 10^{15} \text{ W cm}^{-2}$) laser pulse with solid targets, has been investigated via proton probing techniques. The shocks' structures and related electric field distributions were reconstructed with high spatial and temporal resolution. The experimental results were interpreted within the framework of the nonlinear wave description based on the Korteweg–de Vries–Burgers equation.

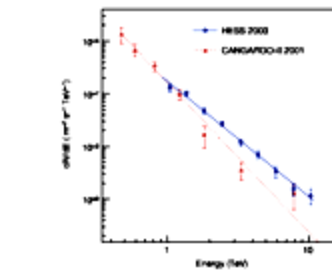
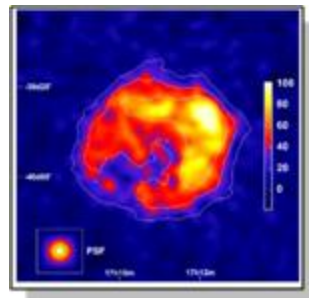
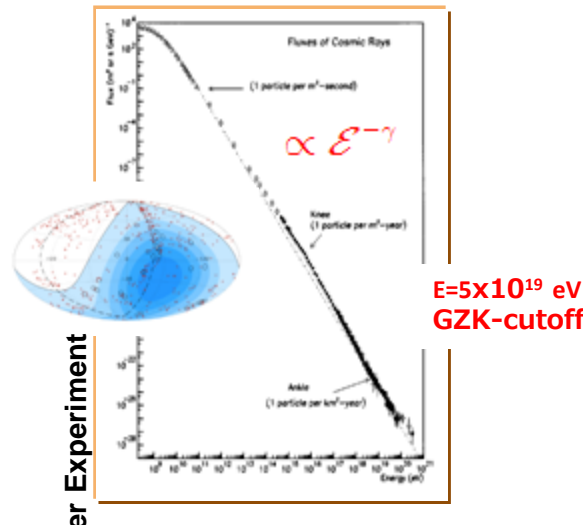


Soliton Shock Wave

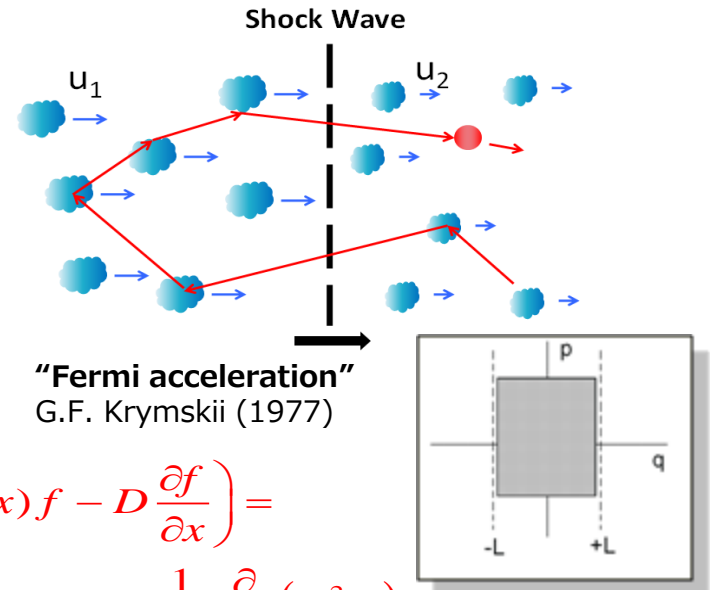


Acceleration at the Shock Wave Front

CR have a power law energy spectrum over several orders of magnitude energy range



The gamma ray image of RX J1713.7-3946 spectrum and gamma ray obtained with the HESS telescope array (Aharonyan et al, 2008)



$$\frac{\partial}{\partial x} \left(u(x) f - D \frac{\partial f}{\partial x} \right) = -\frac{2u_1}{3(\kappa+1)} \delta(x) \frac{1}{p^2} \frac{\partial}{\partial p} (p^2 f)$$

$$u_2 = \frac{\kappa-1}{\kappa+1} u_1 \quad u_1 > u_2$$

$$f(p) = Cp^{-\gamma}$$

$$\gamma = \frac{3u_1}{u_1 - u_2}$$

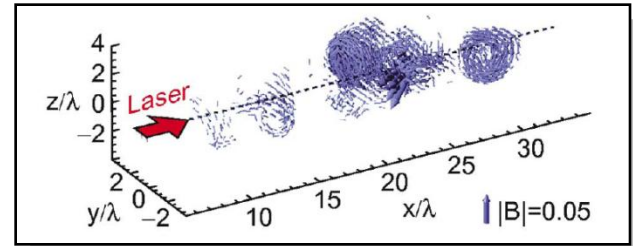
3. Reconnection of Magnetic Field Lines & Vortex Patterns



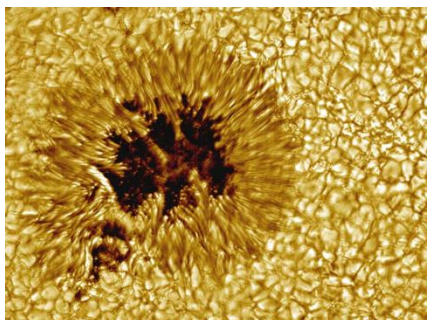
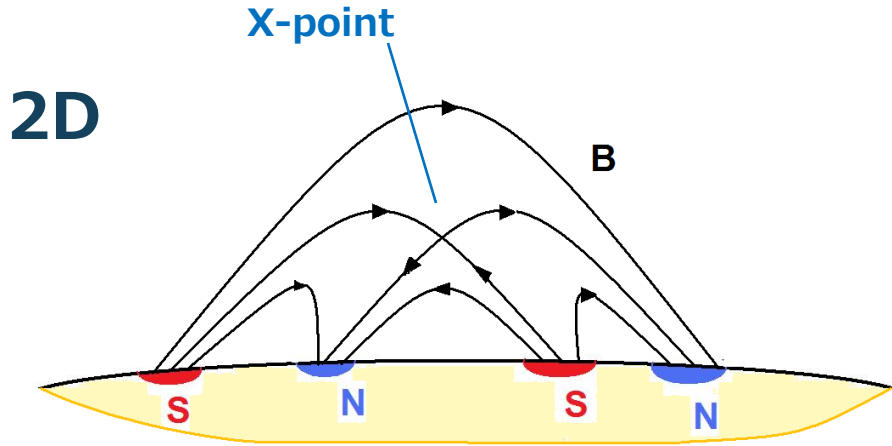
Solar Flare



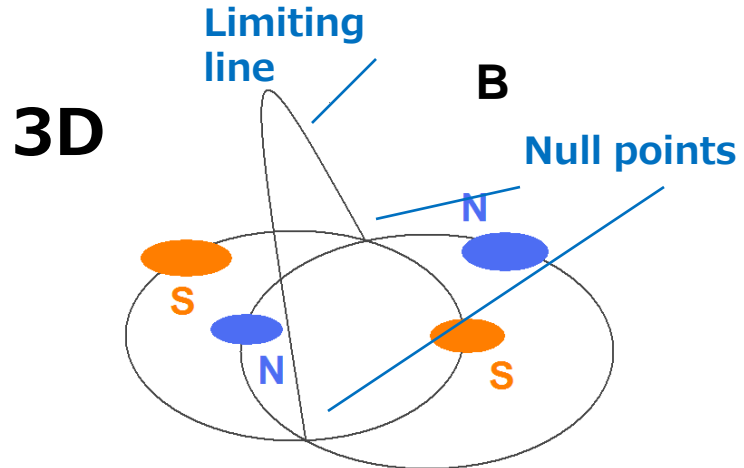
Von Karman vortex row made by the wind over the Pacific island of Guadalupe



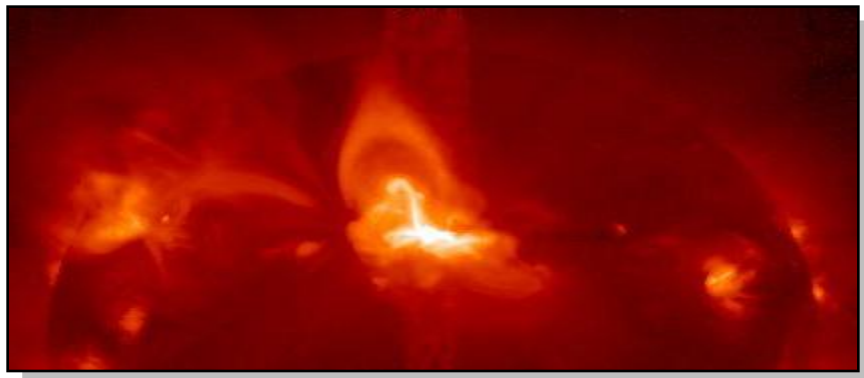
Magnetic (vortex) wake behind the laser pulse:
Esirkepov, et al., 2004



Sunspot



Sweet (1965)



Solar Flare

2D case: The field-line equation reads

$$\frac{dx}{B_x} = \frac{dy}{B_y} = ds$$

Using the relationships

$$B_x = \partial_y A_z - \partial_x F, \quad B_y = -\partial_x A_z - \partial_y F,$$

introducing complex variable $\zeta = x + iy$, complex field and potential

$$B = B_x - iyB_y, \quad \Phi = F - iA_z,$$

we obtain the Hamiltonian equations for the magnetic field lines ($' = d/ds$):

$$\zeta' = -\frac{\partial \Phi}{\partial \zeta}$$

The magnetic field lines are on the surfaces $A_z = \text{constant}$

Local Structure of the Magnetic Field

Near null point we can expand the magnetic field as

$$\mathbf{B}(\mathbf{x}, t) = (\mathbf{B}(0, t) \nabla) \mathbf{x} + \dots$$

Introducing the matrix $\left. \partial B_i / \partial x_j \right|_{x=0} = A_{ij}$, $B_i = A_{ij} x_j$

we write for the magnetic field lines $\frac{dx_i}{ds} = A_{ij} x_j$.

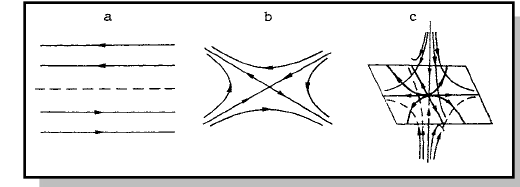
It yields $\det(A_{ij} - \lambda \delta_{ij}) = 0$,

The topology is determined by the eigenvalues λ_α ($\sum_\alpha \lambda_\alpha = 0$)

We have the null surface, null line or null point depending on

$$\lambda_{1,2} = \pm \lambda' \text{ or } \lambda_{1,2} = \pm i\lambda'' \quad \lambda_3 = 0$$

$$\lambda_{1,2} = \lambda' \pm i\lambda'' \quad \lambda_3 = \lambda'$$



MHD Equations

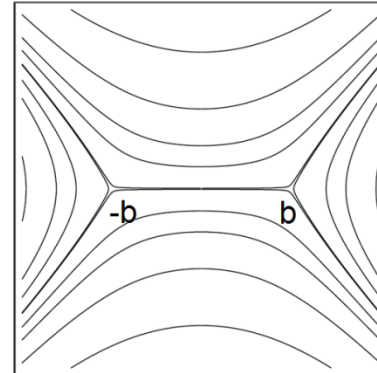
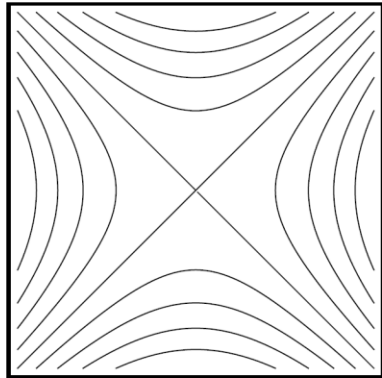
$$\partial_t \rho + \nabla(\rho \mathbf{v}) = 0,$$

$$\partial_t \mathbf{v} + (\mathbf{v} \nabla) \mathbf{v} = \frac{(\nabla \times \mathbf{B}) \times \mathbf{B}}{4\pi\rho},$$

$$\partial_t \mathbf{B} = \nabla \times (\mathbf{v} \times \mathbf{B}) + \nu_m \Delta \mathbf{B},$$

$$\nabla \cdot \mathbf{B} = 0$$

ρ - plasma density; \mathbf{v} - velocity; \mathbf{B} - magnetic field; ν_m - magnetic diffusivity



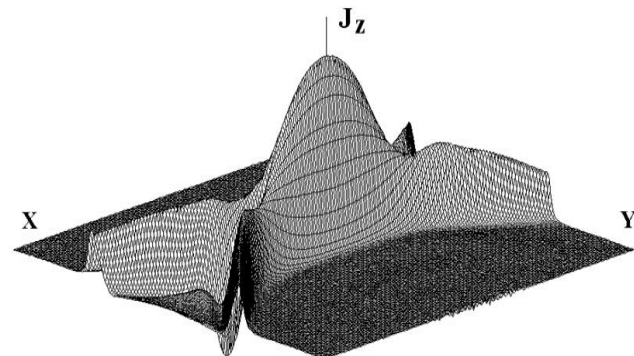
S. I. Syrovatskii, 1971

$$b = \sqrt{4I/hc}$$

$$\Phi = h\zeta^2/2$$

$$\Phi = h \left[\zeta \sqrt{\zeta^2 - b^2} - \ln \left(\zeta - \sqrt{\zeta^2 - b^2} \right) \right]$$

Current sheet near the X-line
of magnetic configuration



SVB, et al, 1996

Magnetic Reconnection in Collisionless Plasmas

In collisionless multispecies plasmas the **curl** of the canonical momentum

$$\mathbf{p}_\alpha = m_\alpha \mathbf{v}_\alpha + (e_\alpha / c) \mathbf{A}$$

is frozen in the corresponding flow velocity

$$\partial_t \nabla \times \mathbf{p}_\alpha = \nabla \times [\mathbf{v}_\alpha \times \nabla \times \mathbf{p}_\alpha]$$

The electron magnetohydrodynamics considers the dynamics of just the electrons, the ions are assumed to be at rest and the quasineutrality condition is fulfilled. The electron velocity is related to the magnetic field as

$$\mathbf{v}_e = -(c / 4\pi n_e) \nabla \times \mathbf{B}$$

with constant plasma density $n_e = n_i$. It yields

$$\partial_t (\mathbf{B} - \Delta \mathbf{B}) = \nabla \times [(\nabla \times \mathbf{B}) \times (\mathbf{B} - \Delta \mathbf{B})]$$

In the linear approximation EMHD describes the whistler waves

The EMHD equations can be written as

$$\partial_t \boldsymbol{\Omega} = \nabla \times [(\nabla \times \mathbf{B}) \times \boldsymbol{\Omega}]$$

Here the generalized vorticity

$$\boldsymbol{\Omega} = \mathbf{B} - \Delta \mathbf{B} = \nabla \times (\mathbf{A} - \Delta \mathbf{A}) = \mathbf{B} + \nabla \times \mathbf{v}$$

is frozen into the electron fluid motion.

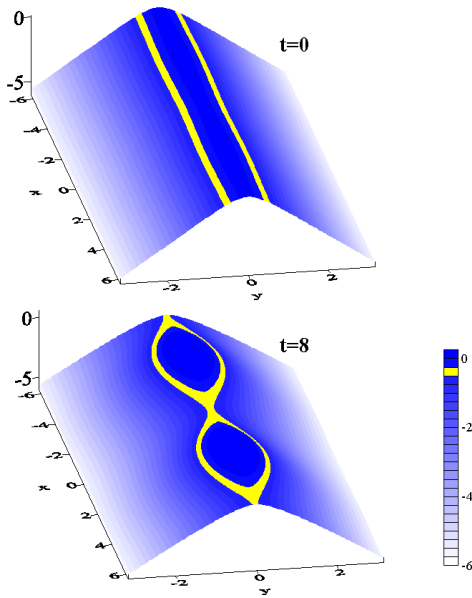
We consider the magnetic field given by

$$\mathbf{B} = \nabla \times (A_{\parallel} \mathbf{e}_z) + B_{\parallel} \mathbf{e}_z$$

The magnetic field pattern in the x, y plane is determined by

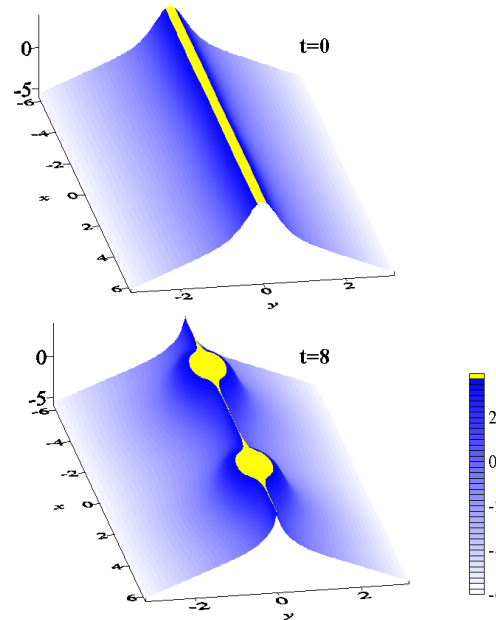
$$A_{\parallel}(x, y, t) = \text{const}$$

Magnetic field



$$A_{||} = \text{const}$$

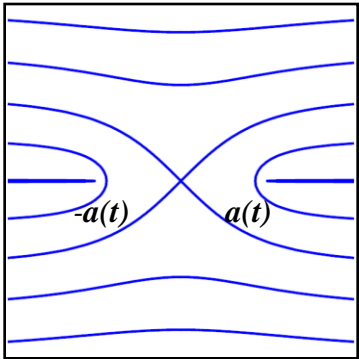
Generalized vorticity



$$A_{||} - \Delta A_{||} = \text{const}$$

K.Avinash, SVB, T.Esirkepov, P.Kaw, F.Pegoraro, P.Sasorov, A.Sen,
Forced Magnetic Field Line Reconnection in Electron Magnetohydrodynamics.
Physics of Plasmas 5, 2946 (1998)

Charged Particle Acceleration



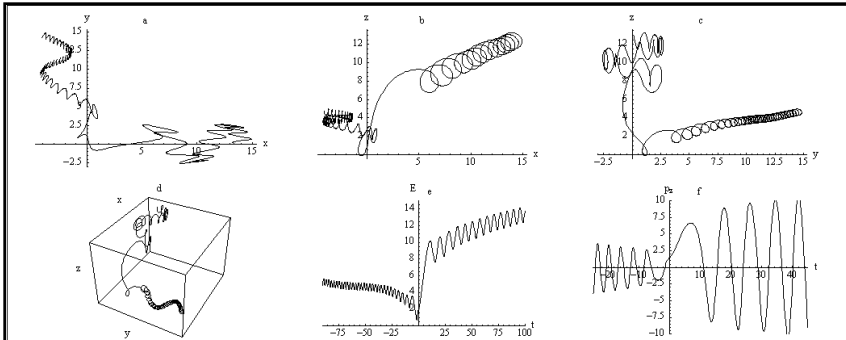
In the vicinity of the X-line, the magnetic field is described by

$$B(\zeta, t) = B_0 \frac{\zeta}{\sqrt{a^2(t) - \zeta^2}} \approx B_0 \frac{\zeta}{a(t)}$$

and the electric field is given by

$$\Phi(\zeta, t) = B_0 \sqrt{a^2(t) - \zeta^2}$$

$$E(\zeta, t) = -B_0 \frac{a(t) \dot{a}(t)}{c \sqrt{a^2(t) - \zeta^2}} \approx \frac{\dot{a}(t)}{c} B_0$$



The energy spectrum of fast particles is given by

$$\frac{d\mathcal{N}(\mathcal{E})}{d\mathcal{E}} \propto \exp\left(-\sqrt{\frac{2\mathcal{E}}{m\dot{a}^2}}\right)$$

Electron Vortices behind the Laser Pulse

Antisymmetric vortex row

$B_z(x, y)$



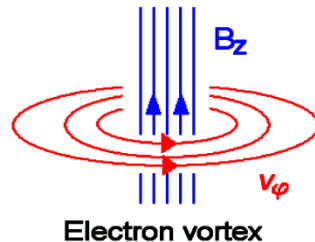
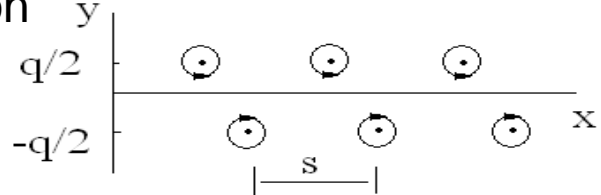
$n_i(x, y)$



L.M.Chen et al., Phys. Plasmas, 14, 040703 (2007)



Vortices described by the Hasegawa-Mima equation



Von Karman vortex row
H.Lamb, Hydrodynamics, 1947

Interacting Point Vortices

As we know $\nabla \times (\mathbf{p} - e\mathbf{A}/c)$ is frozen:

$$(\partial_t + \mathbf{e}_z \times \nabla B \cdot \nabla)(\Delta B - B) = 0$$

Discret vortices are described by equation $\Omega = \Delta B - B = \sum_j \Gamma_j \delta(\mathbf{r} - \mathbf{r}_j(t))$

its solution gives for the magnetic field $B = \sum_j B_j(\mathbf{r}, \mathbf{r}_j(t)) = -\sum_j \frac{\Gamma_j}{2\pi} K_0(|\mathbf{r} - \mathbf{r}_j(t)|)$

and the velocity of j-th vortex is

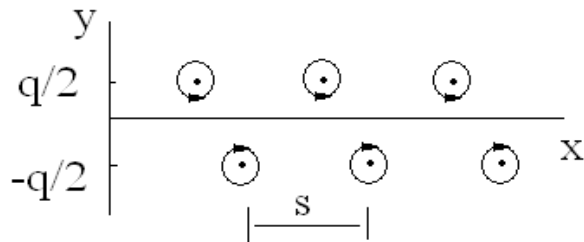
$$\frac{d\mathbf{r}_j}{dt} = \mathbf{e}_z \times \nabla \sum_{k \neq j} B_k(\mathbf{r}_j(t), \mathbf{r}_k(t))$$

The Hamilton equations

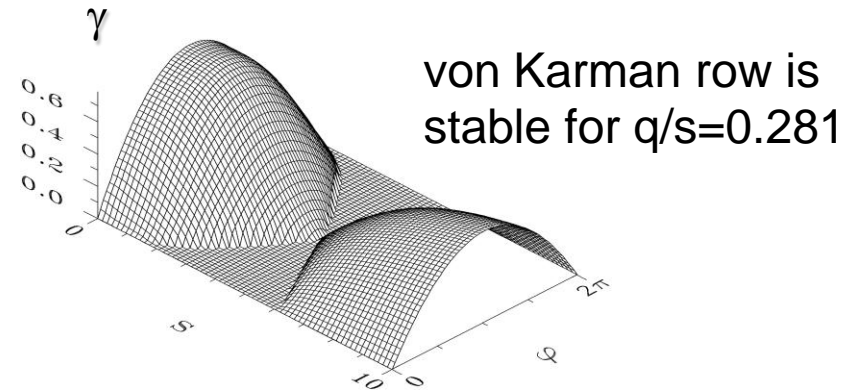
$$\begin{cases} \frac{dx_j}{dt} = \frac{1}{2\pi} \sum_{k \neq j} \Gamma_k \frac{y_k - y_j}{|\mathbf{r}_j(t) - \mathbf{r}_k(t)|} K_1(|\mathbf{r}_j(t) - \mathbf{r}_k(t)|) \\ \frac{dy_j}{dt} = \frac{1}{2\pi} \sum_{k \neq j} \Gamma_k \frac{x_j - x_k}{|\mathbf{r}_j(t) - \mathbf{r}_k(t)|} K_1(|\mathbf{r}_j(t) - \mathbf{r}_k(t)|) \end{cases}$$

Stability Domain

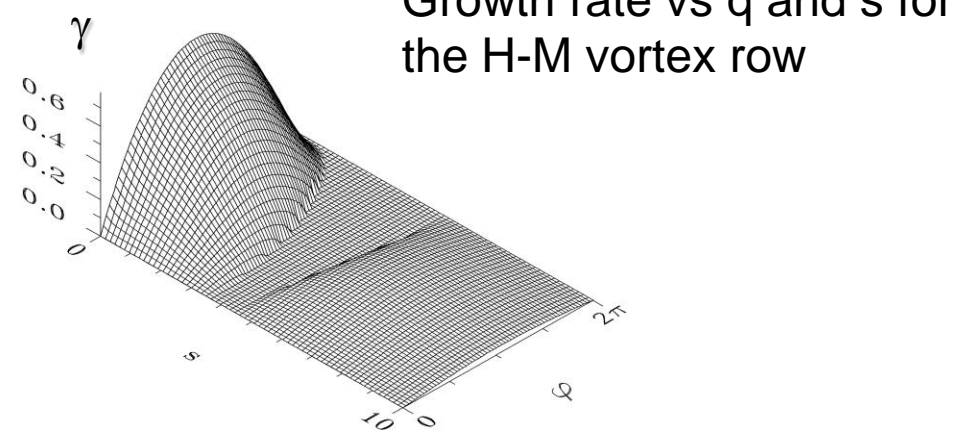
Antisymmetric vortex row



Lyapunov stability in the stability domain was proved

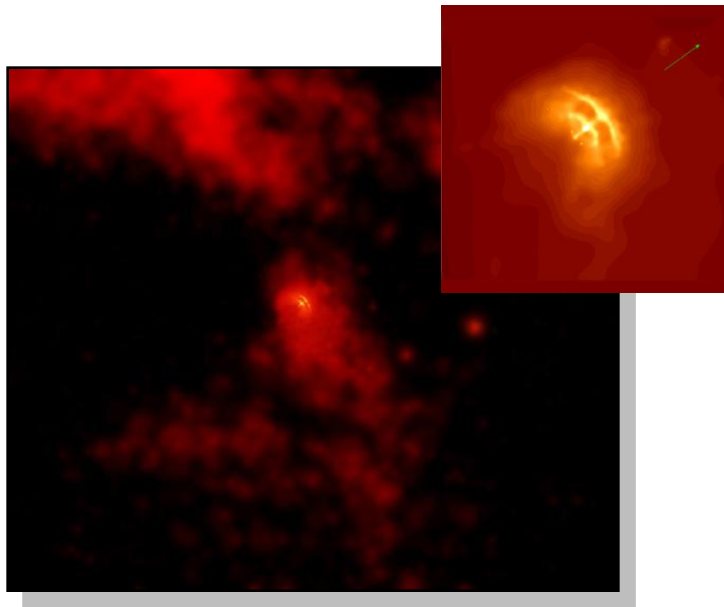


von Karman row is stable for $q/s=0.281$

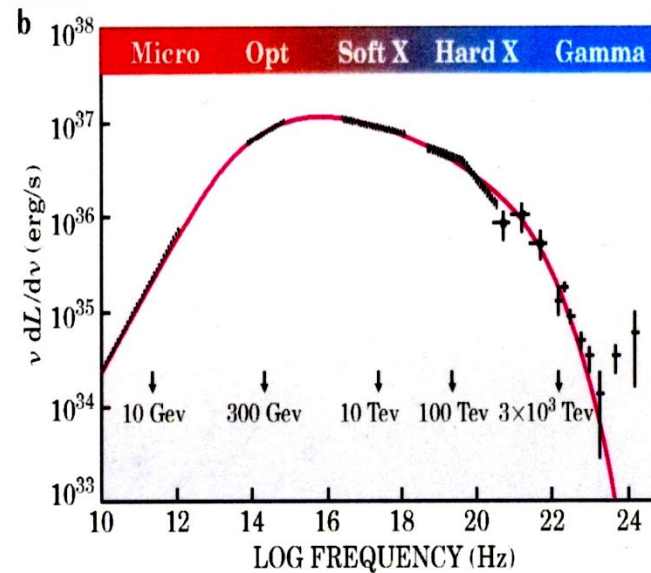
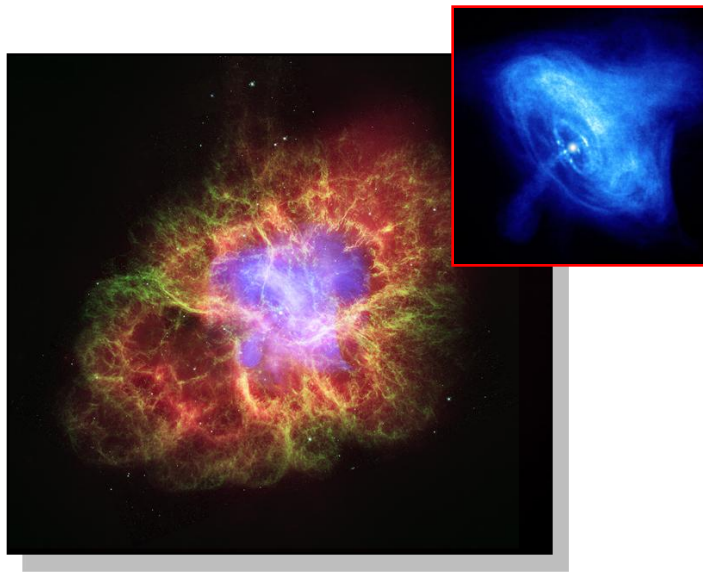


Growth rate vs q and s for the H-M vortex row

4. Relativistic Rotator



PeV γ from Crab Nebula



The Crab Pulsar, lies at the center of the Crab Nebula. The picture combines optical data (red) from the Hubble Space Telescope and x-ray images (blue) from the Chandra Observatory. The pulsar powers the x-ray and optical emission, accelerating charged particles and producing the x-rays.

ON THE PULSAR EMISSION MECHANISMS

1975

V. L. Ginzburg

P. N. Lebedev Physical Institute, Academy of Sciences of the USSR, Moscow, USSR

V. V. Zheleznyakov

Radio-Physical Institute, Gorkii, USSR

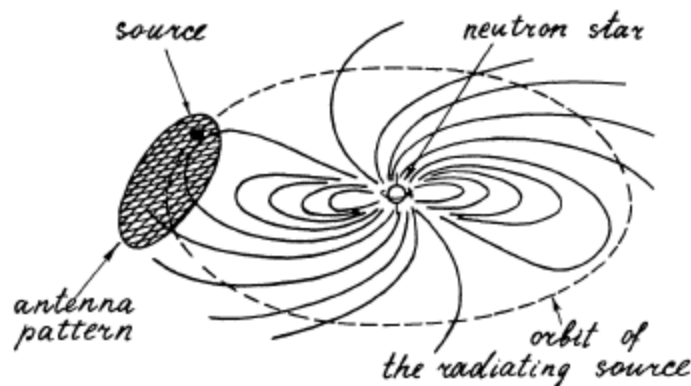
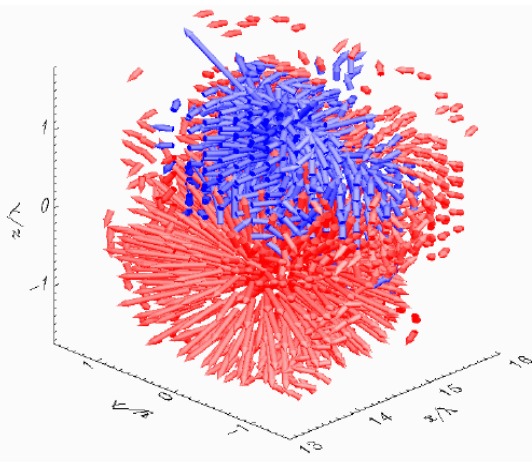


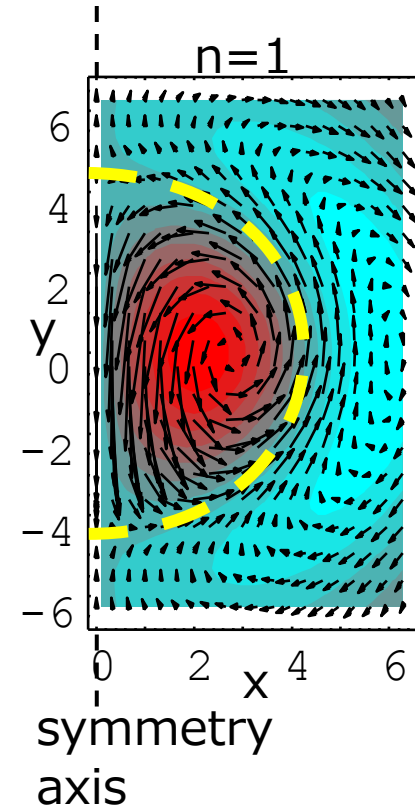
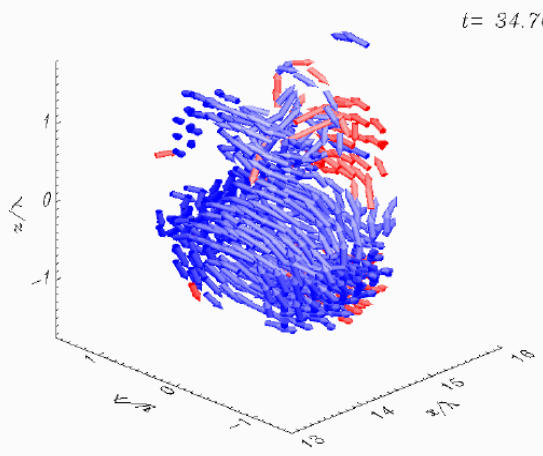
Figure 2 Schematic pulsar model.

Relativistic EM Soliton

E



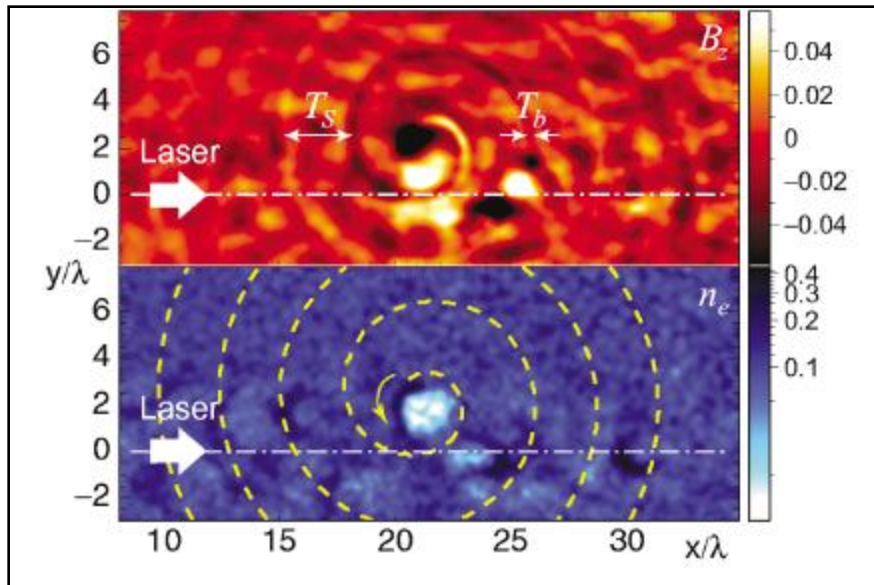
B



E.M. field in a spherical resonator

Circularly Polarized Soliton (3D PIC)

$B_z(x,y)$



$n_e(x,y)$

Classical Electrodynamics Second Edition

JOHN DAVID JACKSON
Professor of Physics, University of California, Berkeley

John Wiley & Sons, Inc., New York • London • Sydney • Toronto

Fig. 14.7 Radiation emitted by a rotating charge

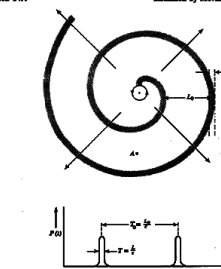


Fig. 14.7 A relativistic particle in periodic motion emits a radial radiation pattern that is observed at the point A due to the short bursts of radiation emitted during $T=2\pi/\omega_r$, occurring at regular intervals $T_0=L/v_r$. The pulse length is given by (14.49), while the interval $T_0=2\pi v_r=2\pi R/c$. For beautiful diagrams of field lines of radiating particles, see R. Y. Chiao, *Am. J. Phys.* 46, 64 (1977).

or Lf in time. From general arguments about the Fourier decomposition of finite wave trains this implies that the spectrum of the radiation will contain appreciable frequency components up to a critical frequency,

$$\omega_c \sim \frac{c}{L} = \left(\frac{\omega_r}{R}\right)^2 \quad (14.50)$$

For circular motion of ρ is the angular frequency of rotation ω_r and over for arbitrary motion it plays the role of a natural radial frequency. Equation (14.50) shows that a relativistic particle emits a broad spectrum of frequencies, up to γ^2



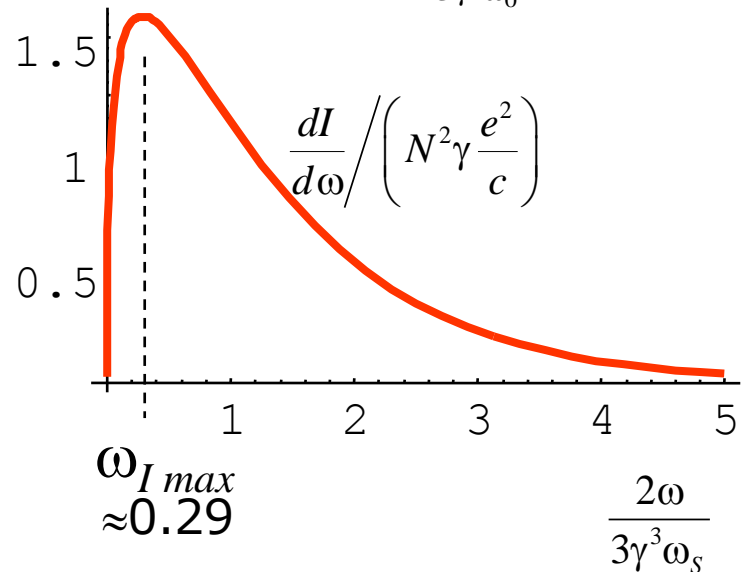
E.M. field energy density

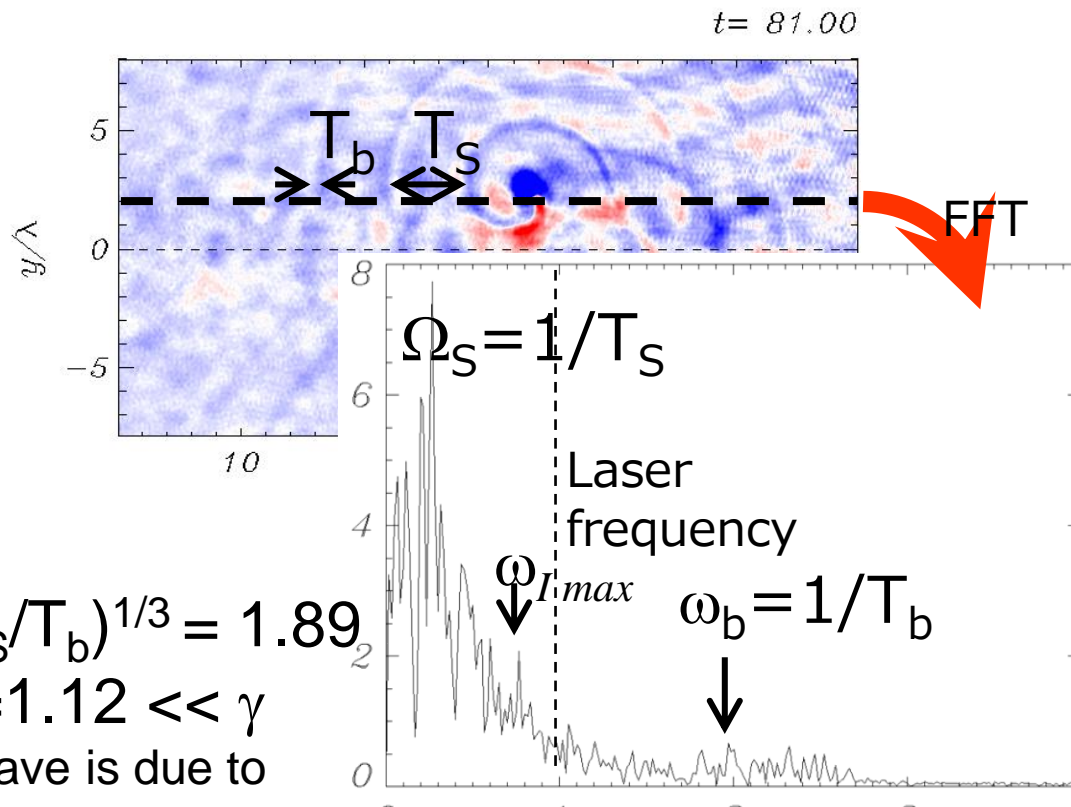
Energy loss by radiation

$$-\frac{d\mathcal{E}}{dt} = \frac{2e^2}{3c} N^2 \omega_0^2 \gamma^2 (\gamma^2 - 1)$$

Frequency distribution of the total energy emitted by coherently rotating electrons

$$\frac{dI}{d\omega} = \sqrt{3} N^2 \gamma \frac{e^2}{c} \frac{2\omega}{3\gamma^3 \omega_0} \int_{\frac{2\omega}{3\gamma^3 \omega_0}}^{\infty} K_{5/3}(\xi) d\xi$$



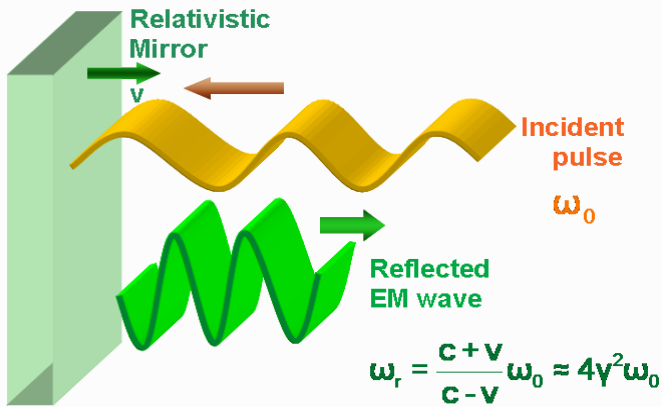


The solitons as the relativistic rotators can model the pulsar radiation under the earth laboratory conditions

5. Flying Mirror for Femto-, Atto-, ... Super Strong Field Science

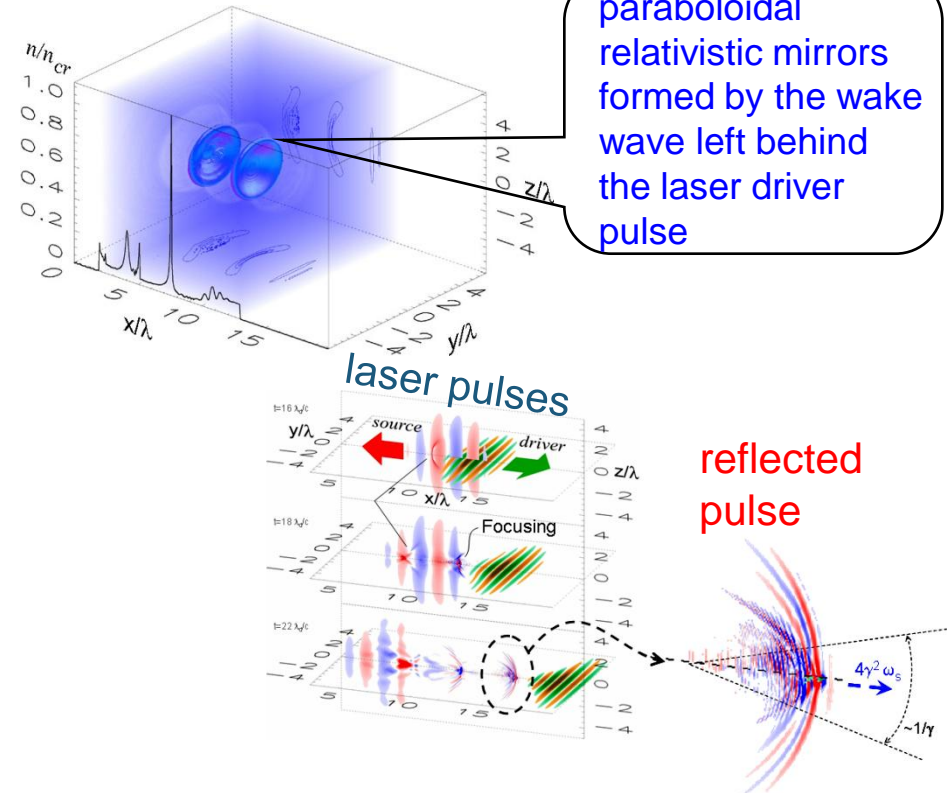


Flying Mirror Concept



A. Einstein, Ann. Phys. (Leipzig) 17, 891 (1905)

Frequency up-shifting and intensification of the light reflected at the relativistic mirror



S. Bulanov, T. Esirkepov, T. Tajima, Phys. Rev. Lett. 91, 085001 (2003)

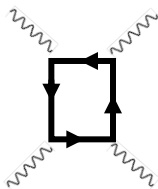
Laser Energy & Power to Achieve the Schwinger Field

The driver and source must carry **10 kJ** and **30 J**, respectively

Reflected intensity can approach **the Schwinger limit** $I_{QED} = 10^{29} W / cm^2$

$$E_{QED} = \frac{m_e^2 c^3}{e\hbar}$$

It becomes possible to investigate such the fundamental problems of nowadays physics, as e.g. the **electron-positron pair creation in vacuum** and the **photon-photon scattering**



$$\mathcal{L} = \frac{1}{16\pi} F_{\alpha\beta} F^{\alpha\beta} - \frac{\kappa}{64\pi} \left[5(F_{\alpha\beta} F^{\alpha\beta})^2 - 14F_{\alpha\beta} F^{\beta\gamma} F_{\gamma\delta} F^{\delta\mu} \right]$$

The **critical power** for nonlinear vacuum effects is

$$\mathcal{P}_{cr} = \frac{45\pi^2}{\alpha} \frac{c E_{QED}^2 \lambda^2}{4\pi}$$

$$\mathcal{P}_{cr} \approx 2.5 \times 10^{24} W$$

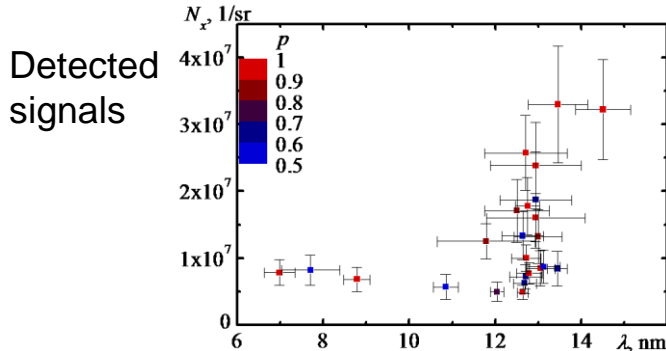
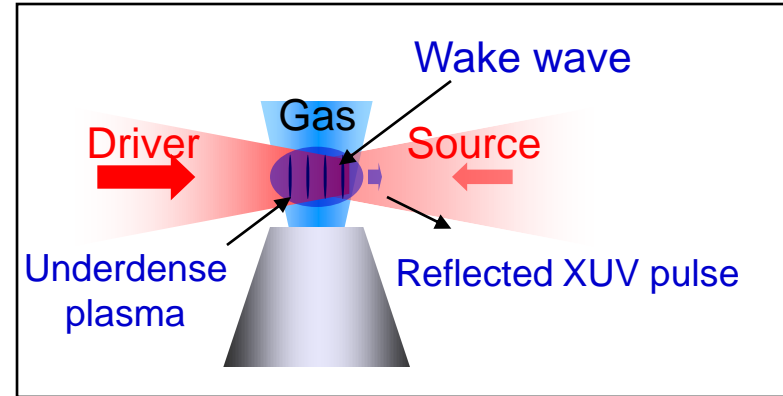
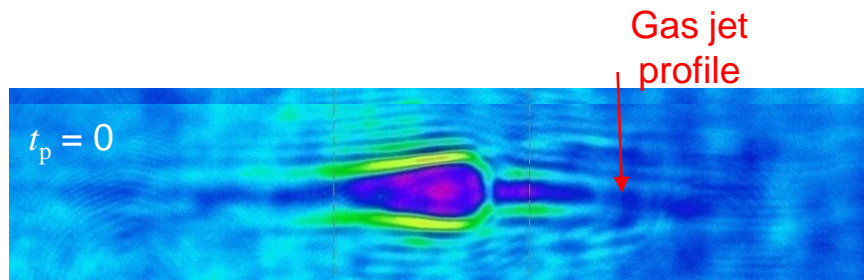
Light compression and focusing with the **FLYING MIRRORS** yields $\mathcal{P} = \mathcal{P}_0 \gamma_{ph}$

for $\lambda_0 = 1\mu m$ $\lambda = \lambda_0 / 4\gamma_{ph}^2$ with $\gamma_{ph} \approx 30$ the driver power

P_{cr}=10 PW

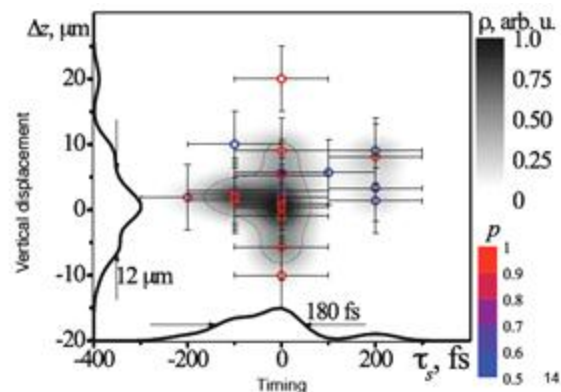
Proof of Principle Experiment

In our experiments, narrow band XUV generation was demonstrated



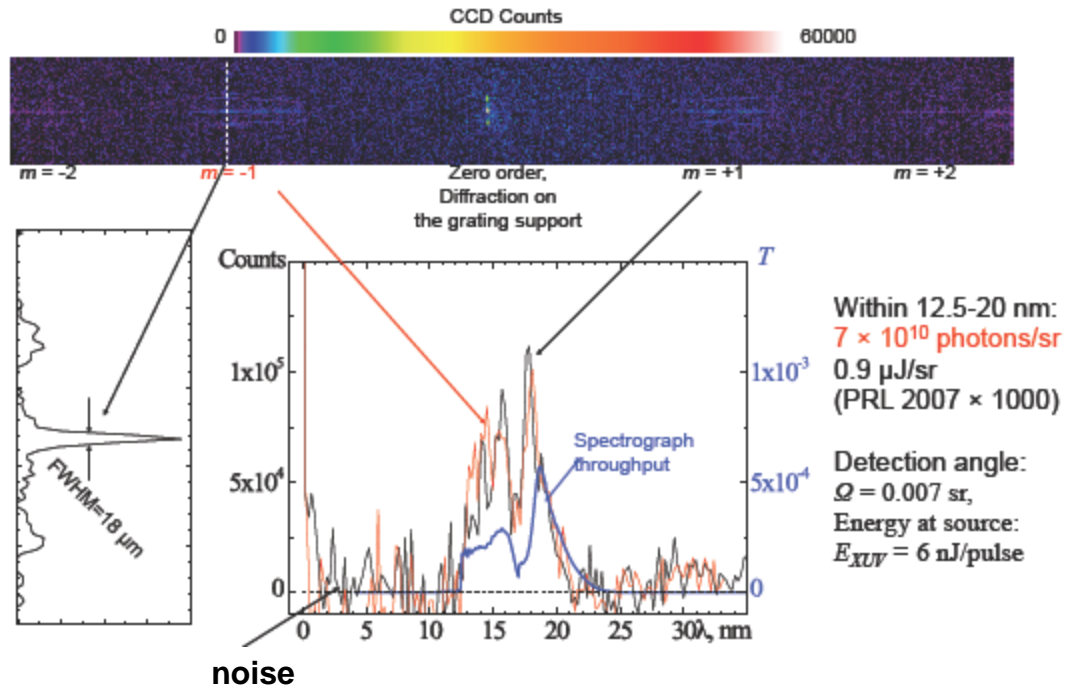
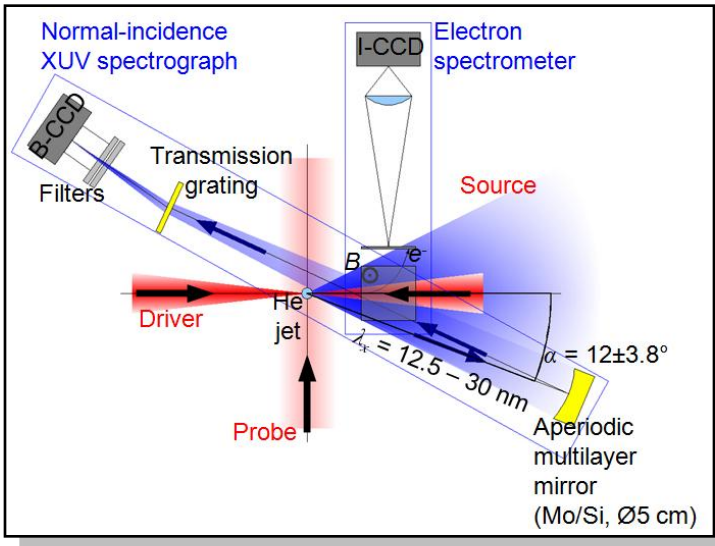
Frequency multiplication

$$\frac{\omega_r}{\omega_s} = 55 \dots 114$$



M. Kando, et al., Phys. Rev. Lett. 99, 135001 (2007);
A. Pirozhkov, et al., Phys. Plasmas 14, 123106 (2007)

Flying Mirror in the Head-On Collision Experiment

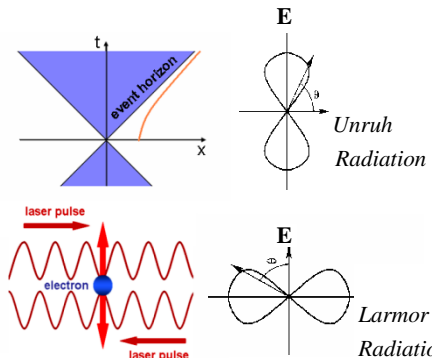


Within 12.5-20 nm:
 $7 \times 10^{10} \text{ photons/sr}$
 $0.9 \mu\text{J/sr}$
(PRL 2007 $\times 1000$)

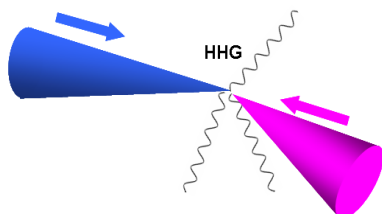
Detection angle:
 $\Omega = 0.007 \text{ sr}$,
Energy at source:
 $E_{XUV} = 6 \text{ nJ/pulse}$

Two head-on colliding laser pulses

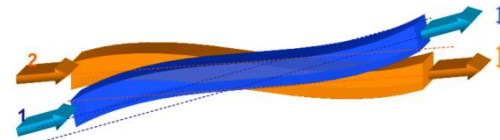
High Field Science



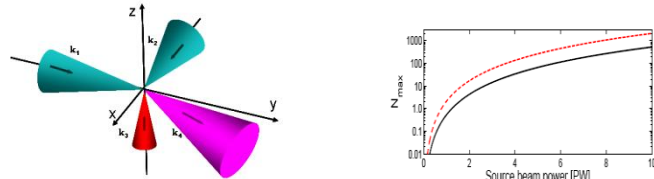
Unruh radiation (Chen&Tajima (1999))



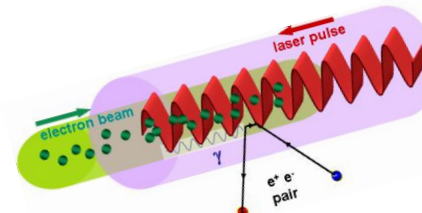
Higher harmonic generation through quantum vacuum interaction (Fedotov & Narozhny (2006); Di Piazza, Keitel)



Birefringent e.m. vacuum (Rozanov (1993))



4-wave mixing (Lundström et al (2006))



Electron-positron pair production in the laser interaction with the electron beam: $e^- + n\gamma \rightarrow \gamma, \gamma + n\gamma' \rightarrow e^+ + e^-$
Bula et al (1996); Burke et al (1997)

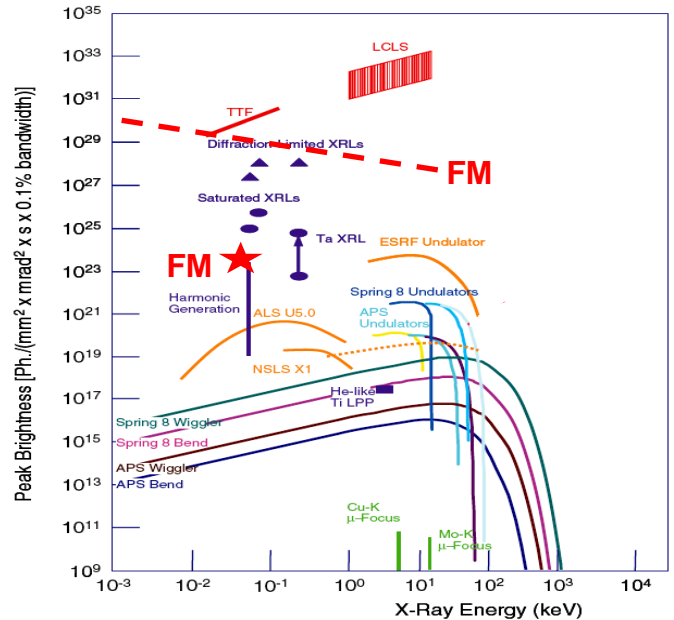
Compact Coherent Ultrafast X-Ray Source

X-ray source	Wavelength	Pulse Duration	Pulse Energy	Mono-chromativity ($\Delta\lambda/\lambda$)	Coherence
XFEL (DESY)	13.8 nm	50 fs	100 μ J	10^{-3}	spatial good
Plasma XRL	13.9 nm	7 ps	10 μ J	10^{-4}	spatial good
Laser plasma	wide spectrum 1 nm – 40 nm	1 ps – 1 ns	10 μ J	$10^{-2} – 10^{-3}$	No
HHG	5 – 200 nm	100 attosec	1 μ J	$10^{-2} – 10^{-3}$	spatial and temporal good
Flying Mirror	0.1 – 20 nm	< 1 fs	1 mJ	$10^{-2} – 10^{-4}$	spatial and temporal good

Predicted by the FM theory parameters of the x-ray pulse compared with the parameters of high power x-ray generated by other sources

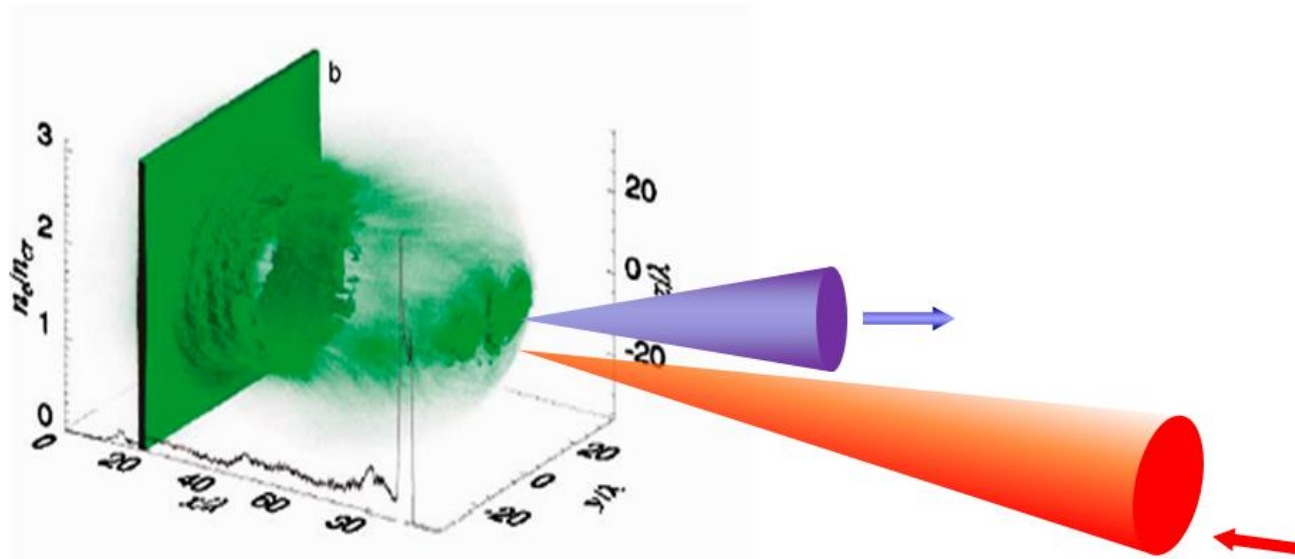
Brightness

$$B = 2 \times 10^{28} \left(\frac{\mathcal{E}_{las}}{1 \text{ J}} \right) \sqrt{\frac{1 \text{ KeV}}{\hbar \omega_\gamma}} \frac{1}{\text{mm}^2 \text{ mrad}^2 0.1\% \text{ bandwidth}}$$

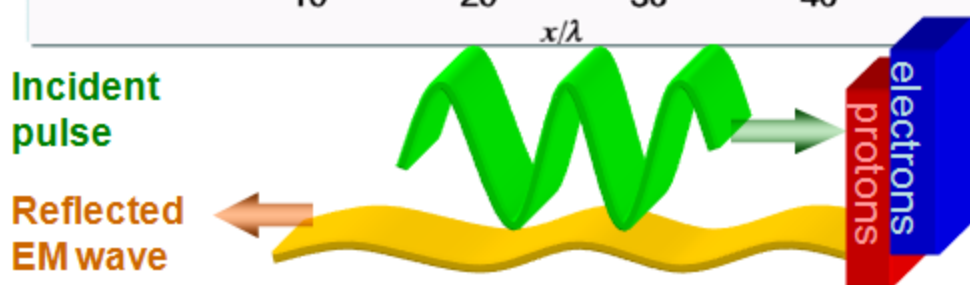
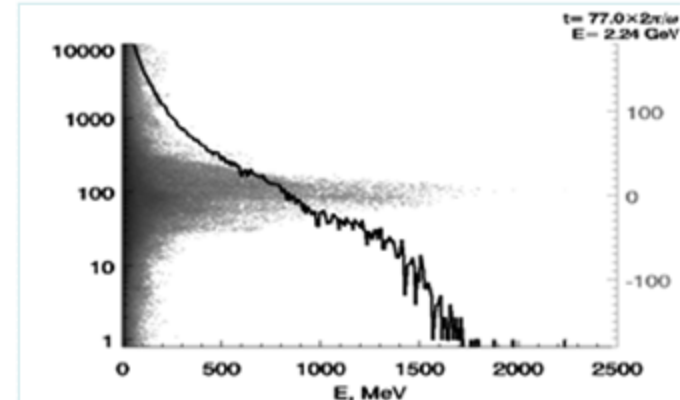
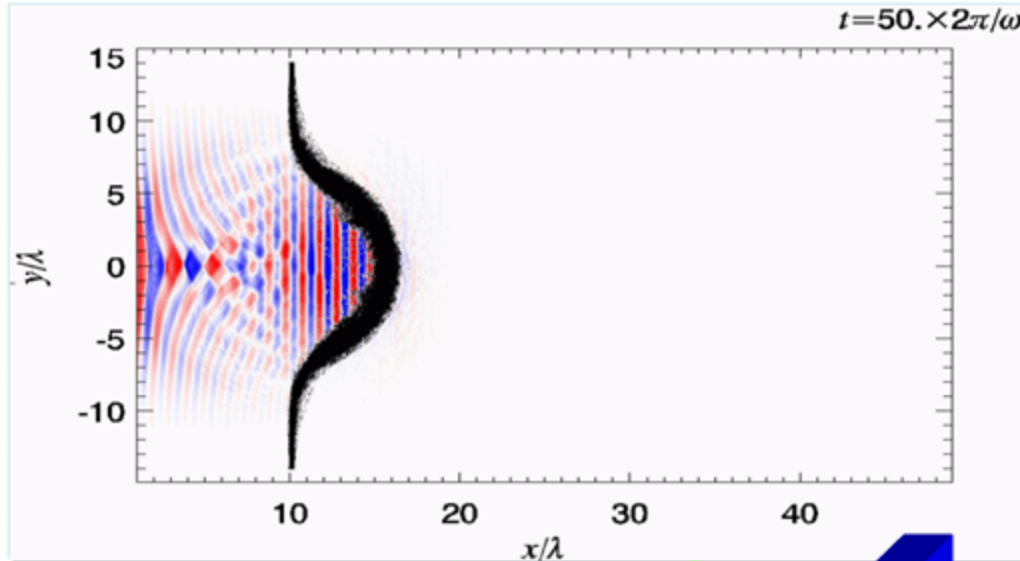


Peak brightness of various light sources

6. Overdense Accelerating Mirror

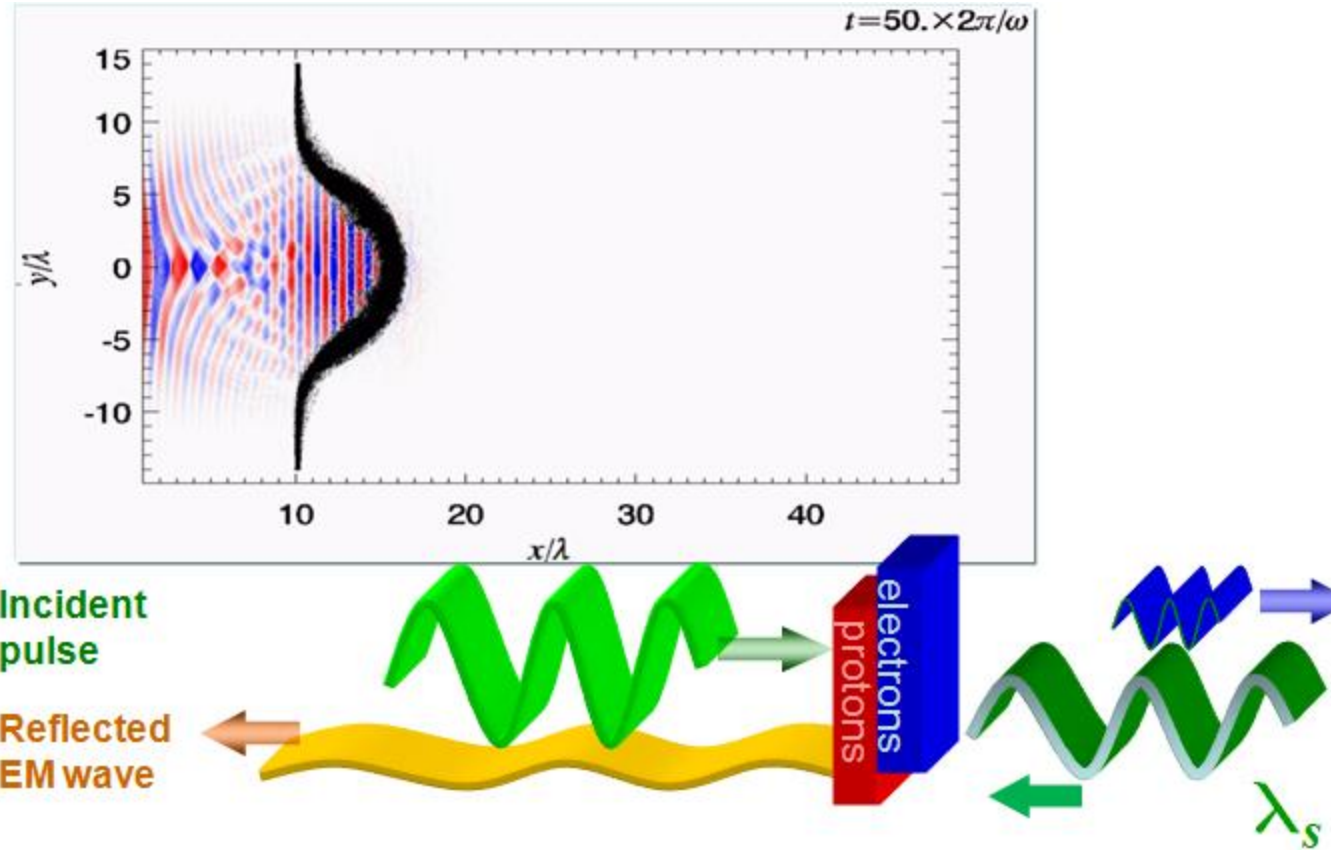


Accelerating mirror

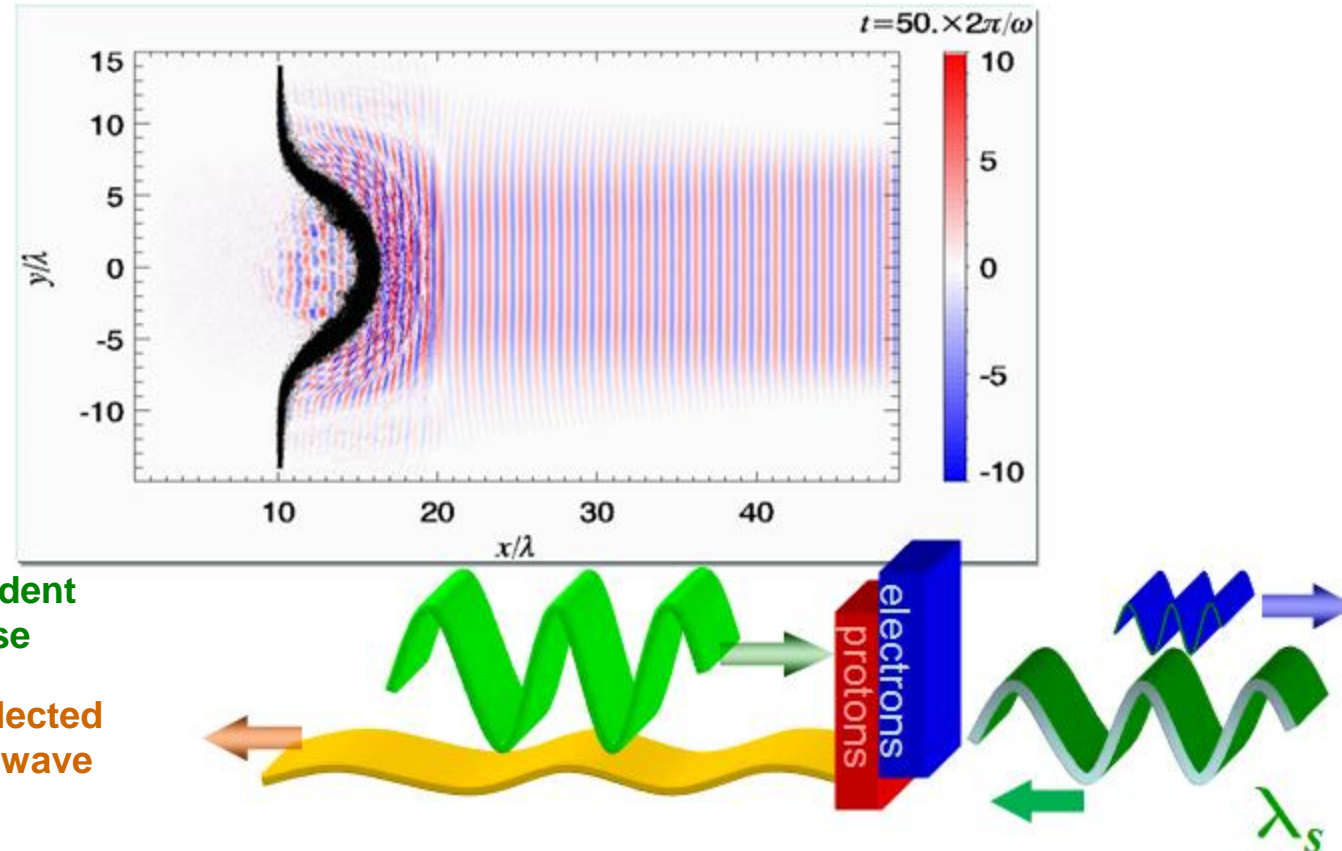


T.Esirkepov, M.Borghesi, SVB, G.Mourou, T.Tajima (2004)
LP or RPDA

Accelerating mirror

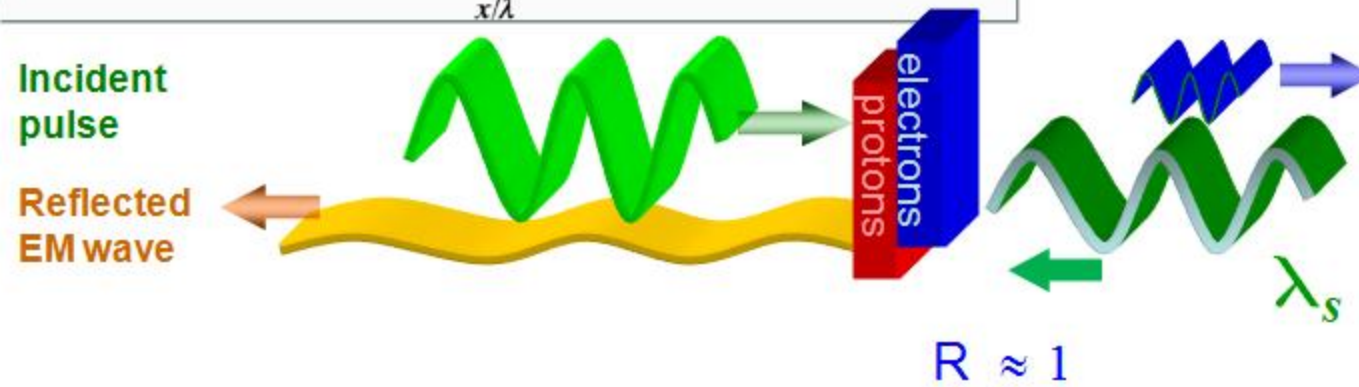
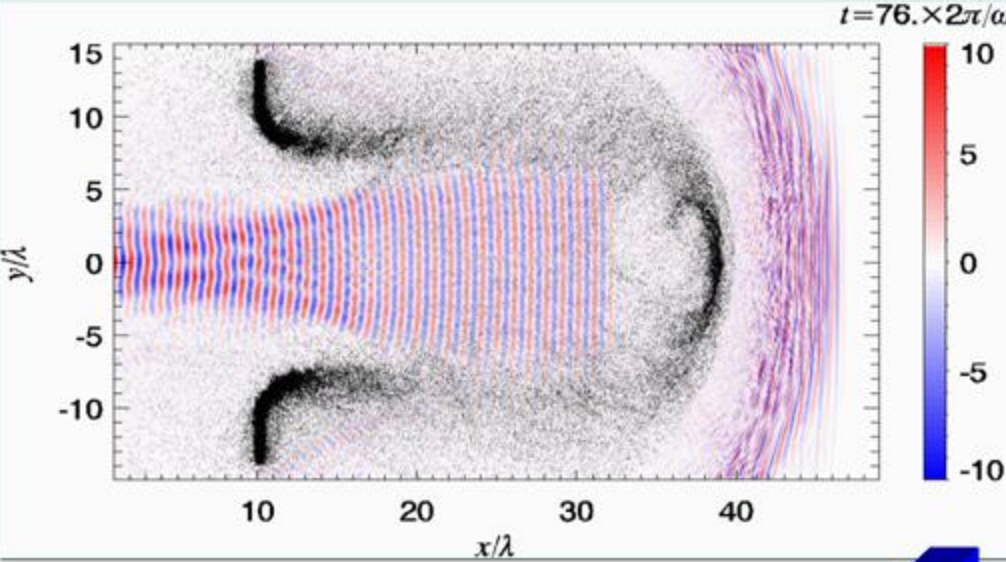


Accelerating mirror

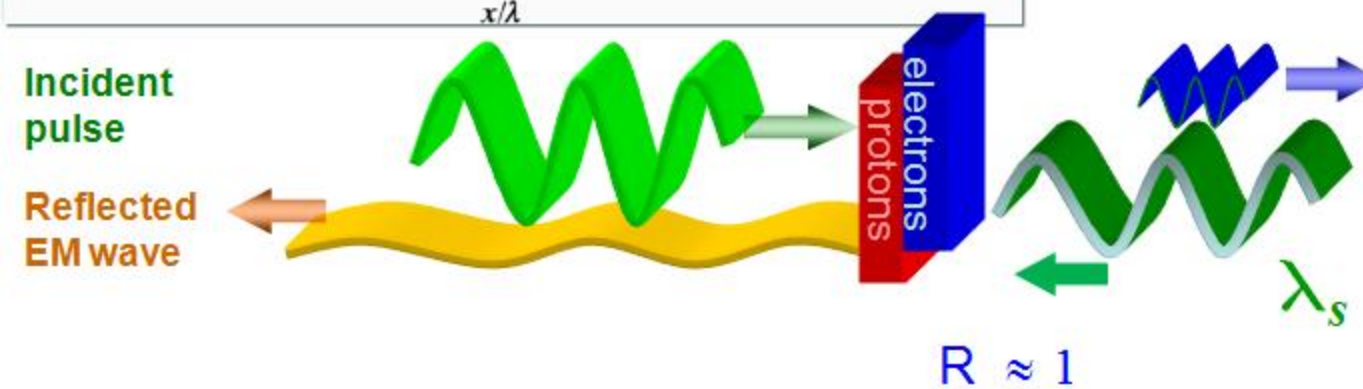
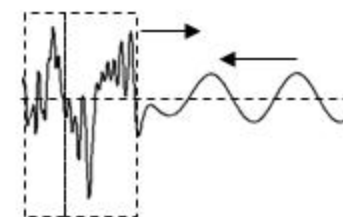
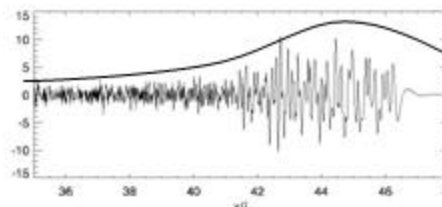
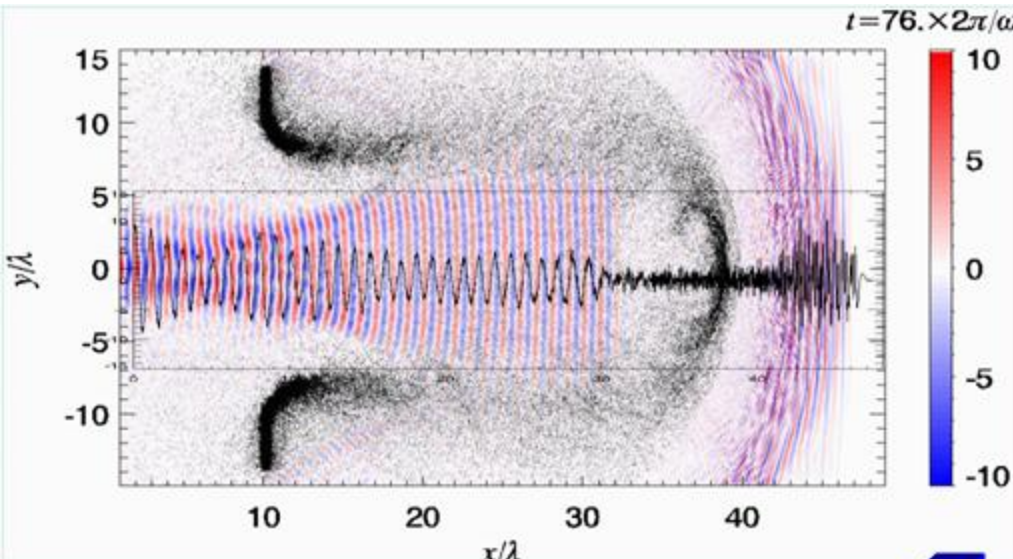


$$\sim \lambda_r \approx \frac{\lambda_s}{4\gamma^2}$$

Accelerating mirror



Laser Piston+Flying Mirror+Oscillating Mirror



Boosted
High Order
Harmonics

$$\omega_n = n \omega \cdot 4 \gamma^2$$

I did not discuss

Weibel Instability

Unipolar Accelerator

Wake Field Acceleration

Buneman Instability.....

Several other realizations of relativistic mirrors

7. Conclusion

- a) Ultra Short Pulse Laser – Matter Interaction has entered the Ultrarelativistic Regime. By this it has opened a new field of Relativistic Laboratory Astrophysics
- b) Laser Piston+Flying Mirror+Oscillating Mirror will provide in a nearest future the instruments for nonlinear vacuum probing and for studying other fundamental problems

Xie Xie

Second International Symposium on Laser-Driven Relativistic Plasmas Applied to Science, Industry and Medicine

Kansai Photon Science Institute, JAEA,
Kizugawa, Kyoto, Japan, January 19 to 23, 2009

supported by KPSI, PMRC, JAEA, ILE Osaka, JSPS ICHEDS, JSPS KAKENHI

Symposium Chair: H. Daido

Program Committee:

Chair – S.V. Bulanov (KPSI, Japan)
V.Yu. Bychenkov (LPI, Russia)
D. Habs (MPQ, Germany)
T. Kawachi (KPSI, Japan)
V. S. Khoroshkov (ITEP, Russia)
H. Kiriyama (KPSI, Japan)
D.K. Ko (GIST, Korea)
C. Ma (FCCC, USA)
K. Mima (ILE, Japan)
J. Mizuki (KPSI, Japan)
G. Mourou (LOA, France)
M. Murakami (HIBMC, Japan)
N. B. Narozhny (MIPE, Russia)
P. Nickles (MBI, Germany)
F. Pegoraro (U. Pisa, Italy)
I.A. Shcherbakov (GPI, Russia)
Z.M. Sheng (SJTU, China)
L. Silva (IPFN, Portugal)
T. Tajima (KPSI, Japan)

Organizing Committee:

Chair – P.R. Bolton (KPSI, Japan)
T.Zh. Esirkepov (KPSI, Japan)
J. Fuchs (ULI, France)
S. Kawanishi (KPSI, Japan)
R. Kodama (U. Osaka, Japan)
K. Kondo (KPSI, Japan)
K. Kurosaka (KPSI, Japan)
K. Moribayashi (KPSI, Japan)
D. Neely (RAL, UK)
H. Nishimura (ILE, Japan)
M. Nishiuchi (KPSI, Japan)
A. Noda (U. Kyoto, Japan)
S. Orimo (KPSI, Japan)
M. Roth (TUD&GSI, Germany)
H. Sakaki (KPSI, Japan)

Topics:

- a) Charged Particle Acceleration
- b) XUV and X-ray Generation
- c) Relativistic Laser Astrophysics
- d) Extreme Field Science
- e) Medical and Industrial Applications



Secretary - Ayako Iwata (kansai-lrpasim@jaea.go.jp)

Webmaster- Toshiki Asai

website - <http://wwwapr.kansai.jaea.go.jp/en/pmrc-sympo2/>